Consecutive visible light-induced electron transfer processes using organic photocatalysts

Speaker: Mengmeng Xu

Supervisor: Dr. Quan Cai

Content

Introduction

Conventional visible light-induced electron transfer

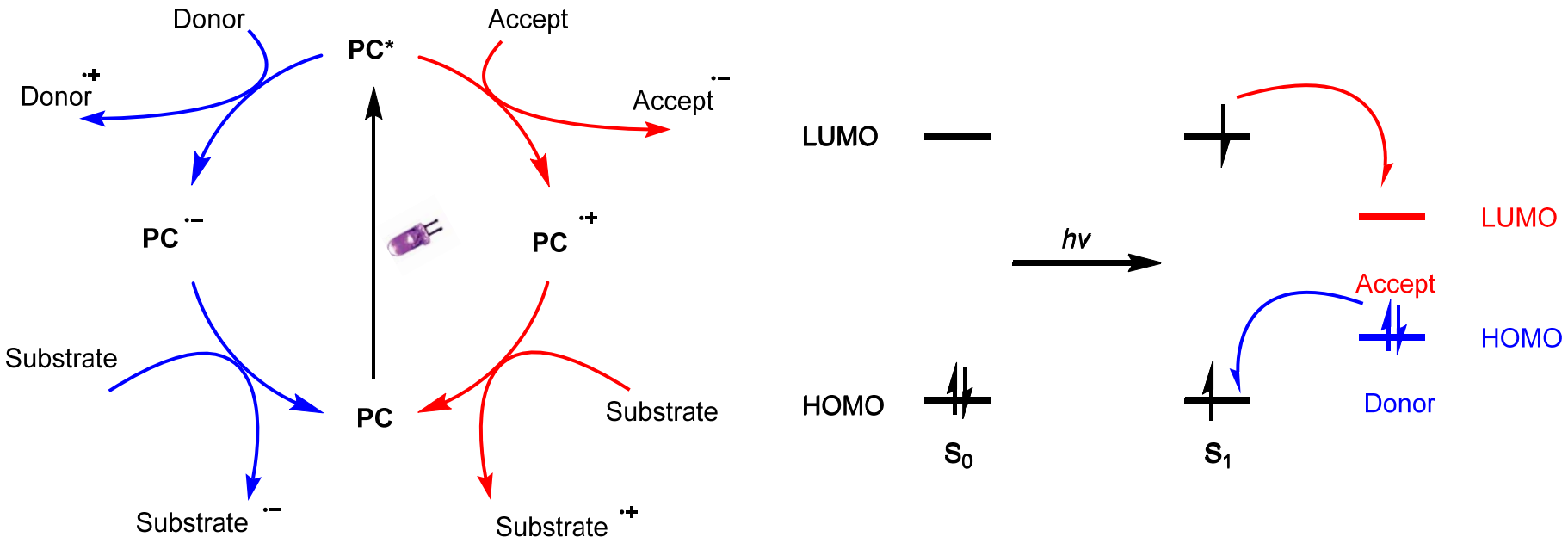

Because this process only accepts one photon, the redox potential of the photocatalyst only ranges from −2 to +2 V.

Schultz, D. M.; Yoon, T. P. *Science* **2014**, *343*, 1239176
Targos, K.; Williams, O. P.; Wickens Z. K. *J. Am. Chem. Soc.* **2021**, *143*, 4125

Introduction

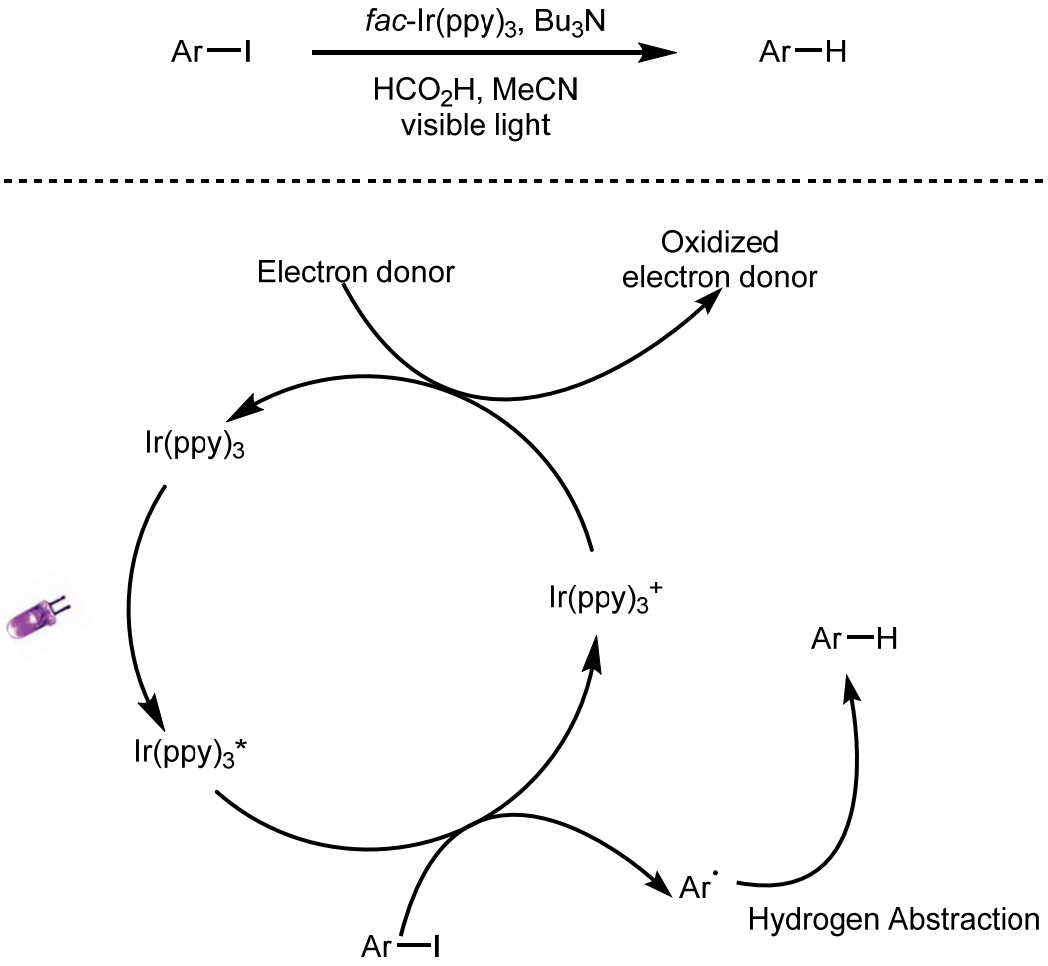

The reduction potential of the excited $Ir(ppy)_3$ is only −1.7 V, which can only reduce specific aryl iodides and can't reduce aryl bromides and chlorides at all.

Nguyen, J. D.; D'Amato, E. M.; Narayanam, J. M. R.; Stephenson, C. R. J. *Nat. Chem.* **2012**, *4*, 854

Introduction

Consecutive visible light-induced electron transfer

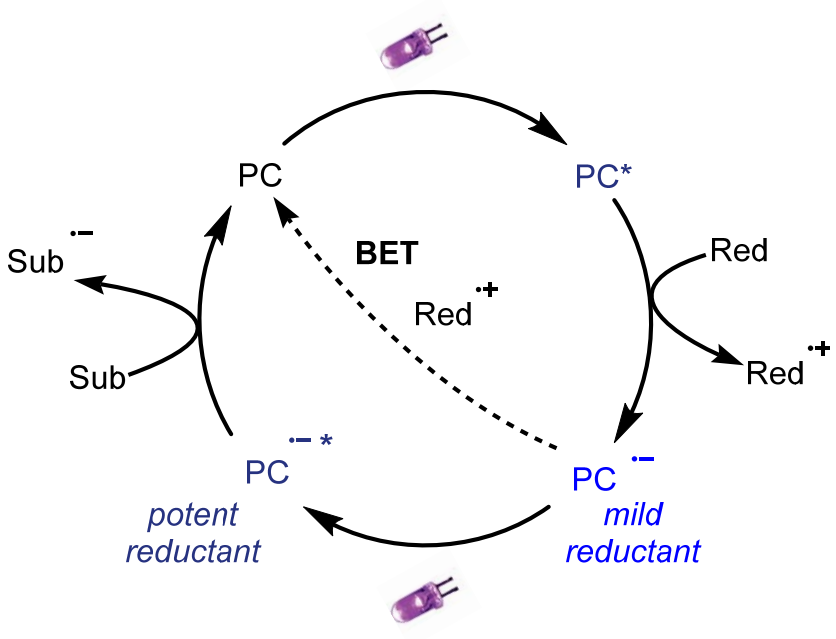

Reductions driven by ConPET

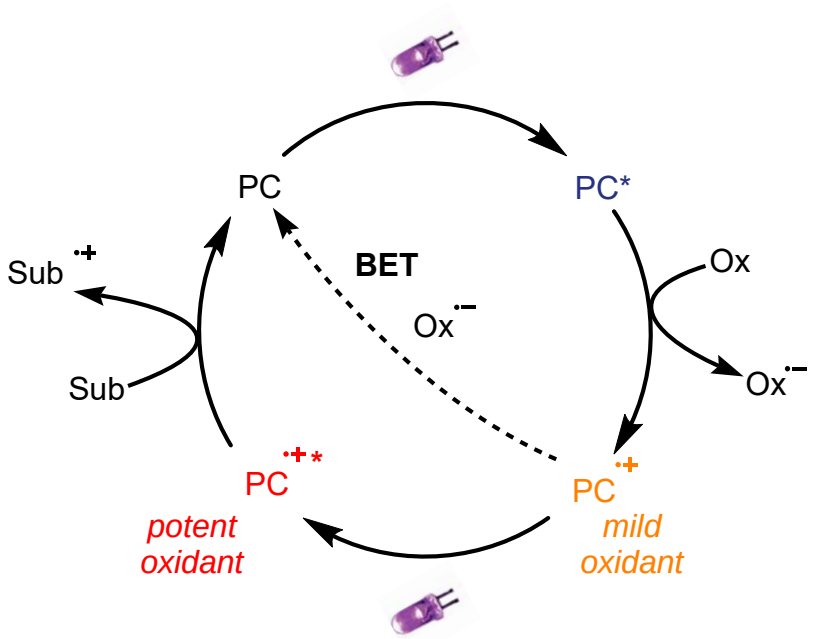

Oxidations driven by ConPET

The redox potential increases because the photocatalyst has absorbed the energy of two photons. This advantage grants ConPET strategy a broader scope of substrates than Conventional PET. Hence, ConPET is more promsing in synthetic applications

Targos, K.; Williams, O. P.; Wickens, Z. K. *J. Am. Chem. Soc.* **2021**, *143*, 4125

Introduction

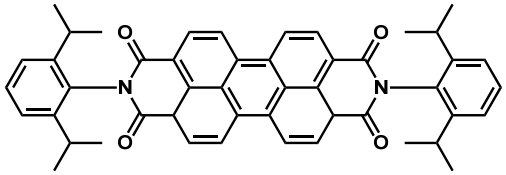

perylene diimide (**PDI**)

König Burkhard
Science **2014**, 725

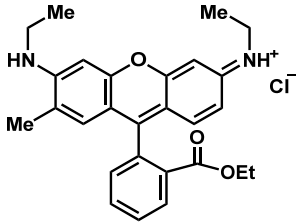

Rh-6G

König Burkhard
ACIE, **2016**, *55*, 7676

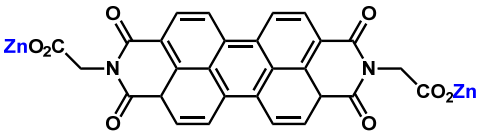

ZnPDI

Duan Chunying
JACS, **2016**, *138*, 3958

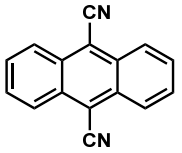

dicyanoanthracene (**DCA**)

Pérez-Ruiz Raul
Chem. Eur. J. **2018**, *24*, 105

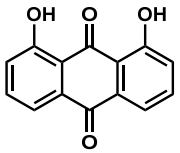

dihydroxyanthraquinone (**Aq-OH**)

König Burkhard
Eur. J. Org. Chem. **2018**, 34

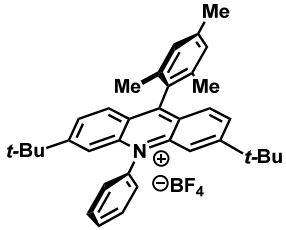

Mes-Acr-BF_4

Nicewicz David A.
Nature **2020**, 76

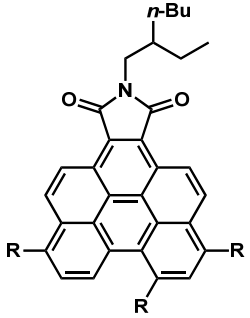

Benzo[ghi]perylene (**BPI**)

Miyake Garret M.
JACS, **2020**, *142*, 13573

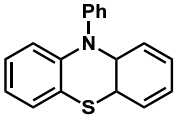

N-phenylphenothiazine (**PTH**)

ChemCatChem ***2018****, 10,* 2955;
ACIE, **2020**, *59*, 300;
JACS, **2021***, 143,* 4125

Content

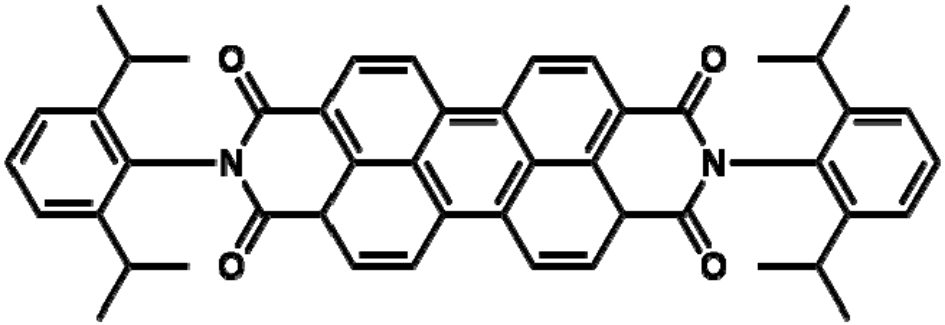

perylene diimide (**PDI**)

König Burkhard
Science **2014**, 725

Reductions driven by ConPET processes

The spectrum of **PDI**

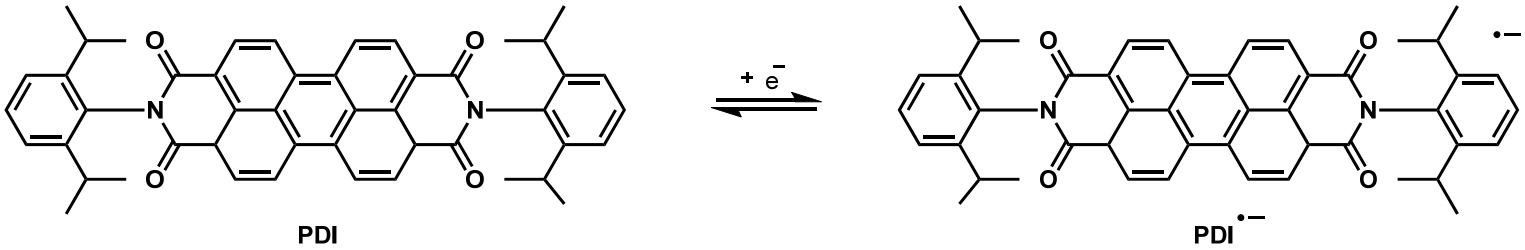

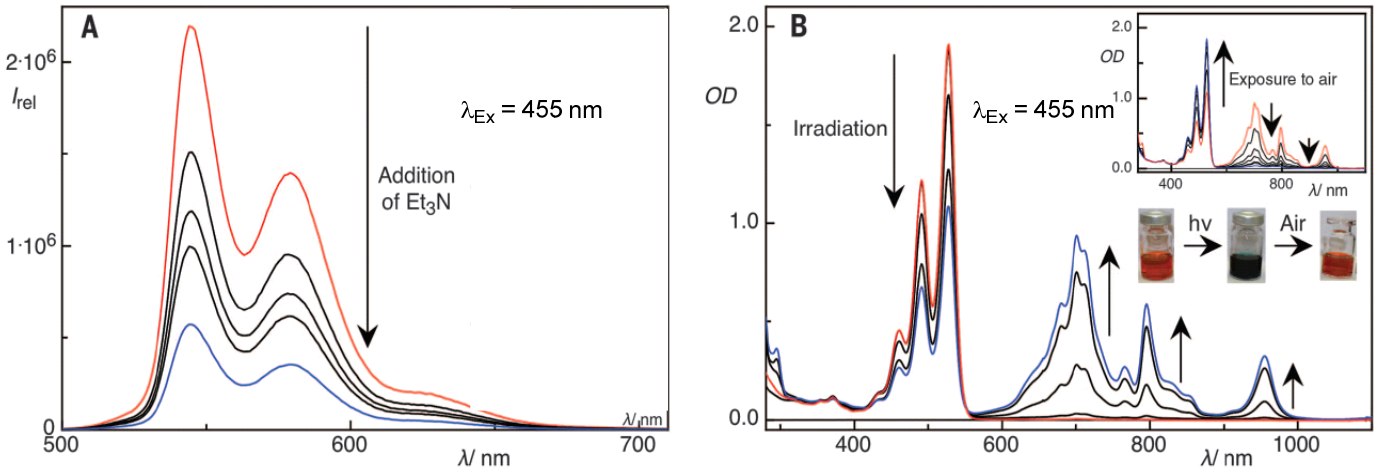

A: Changes in the fluorescence spectra of **PDI** upon successive addition Et_3N in DMF;

B: Changes in the absorption spectra of **PDI** in the presence of Et_3N.

The reduction potential of **PDI**$^{\bullet-}$ is only −0.37 V, which is not enough to reduce the aryl halide.

Ghosh, I.; Ghosh, T.; Bardagi, J. I.; König, B. *Science* **2014**, *346*, 725

Reductions driven by ConPET processes

Control experiments

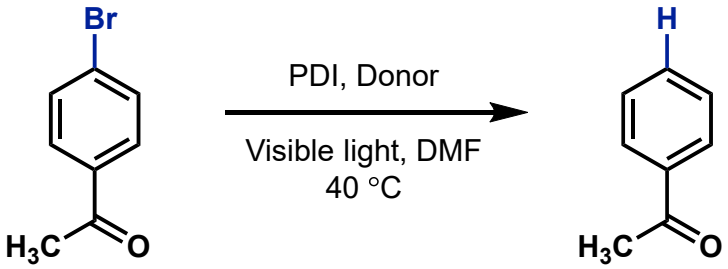

Entry	PDI (mol %)	Donor (equiv)	Reaction condition	Time (h)	Yield (%)
1	5	Et_3N (8)	455 nm, N_2	4	82
2	5	Et_3N (8)	Dark, N_2	4	0
3	-	-	455 nm, N_2	4	0
4	5	-	455 nm, N_2	4	14
5	-	Et_3N (8)	455 nm, N_2	4	0
6	5	Et_3N (8)	455 nm, Air	4	5

Ghosh, I.; Ghosh, T.; Bardagi, J. I.; König, B. *Science* **2014**, *346*, 725

Reductions driven by ConPET processes

Dehalogenation

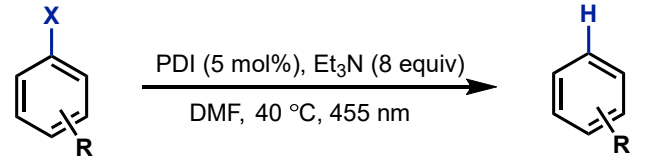

Aryl iodides

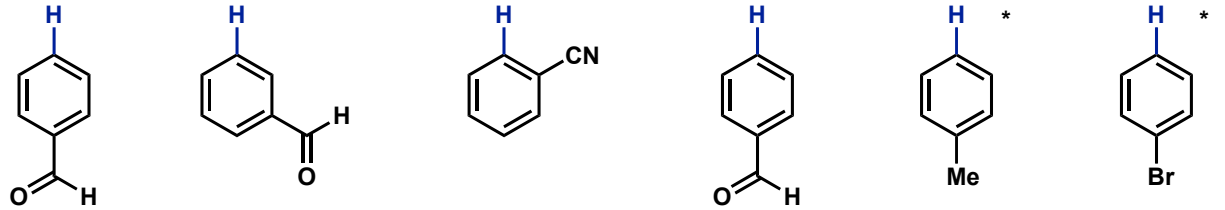

98%, 5 h | 94%, 3 h | 98%, 4 h | 63%, 6 h | 77%, 3 h | 45%, 48 h

Aryl bromides

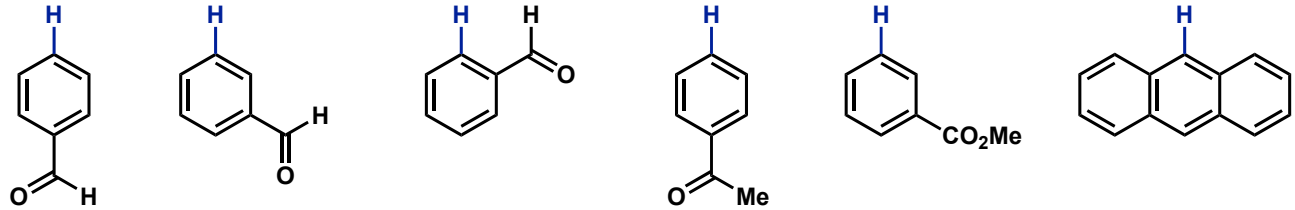

98%, 3 h | 35%, 48 h | 86%, 5 h | 82%, 4 h | 92%, 3 h | 54%, 2 h

Aryl chlorides

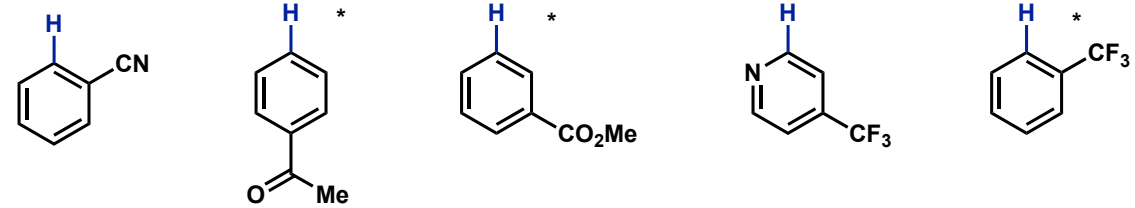

90%, 8 h | 70%, 48 h | 52%, 48 h | 91%, 16 h | 64%, 46 h

* 10 mol% catalyst and 16 equiv of Et_3N were employed.

Ghosh, I.; Ghosh, T.; Bardagi, J. I.; König, B. *Science* **2014**, *346*, 725

Reductions driven by ConPET processes

Arylation reaction

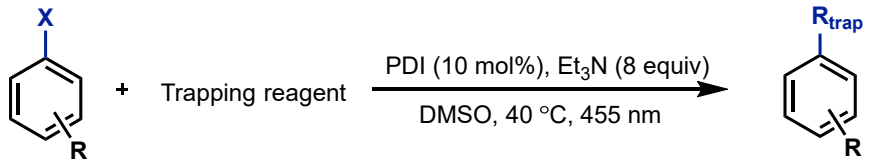

Aryl iodides

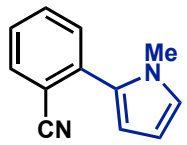

72%, 22 h

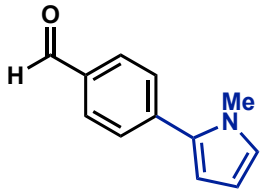

52%, 24 h

Aryl bromides

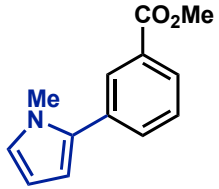

60%, 20 h

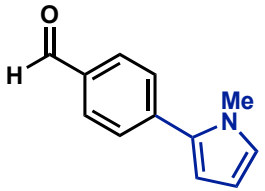

67%, 24 h

Aryl bromides

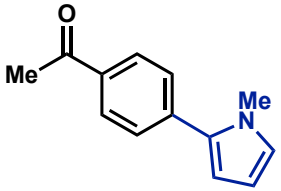

64%, 24 h

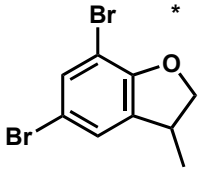

28%, 48 h

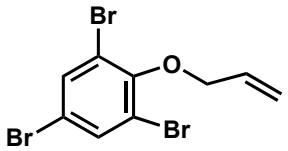

5-exo-trig

Aryl chlorides

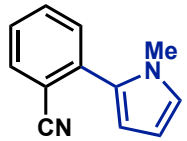

70%, 12 h

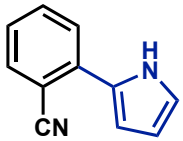

61%, 16 h

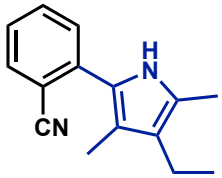

71%, 14 h

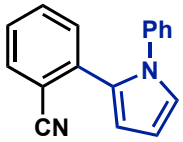

74%, 19 h

* Reaction was performed in DMF.

Ghosh, I.; Ghosh, T.; Bardagi, J. I.; König, B. *Science* **2014**, *346*, 725

Reductions driven by ConPET processes

Mechanism exploration

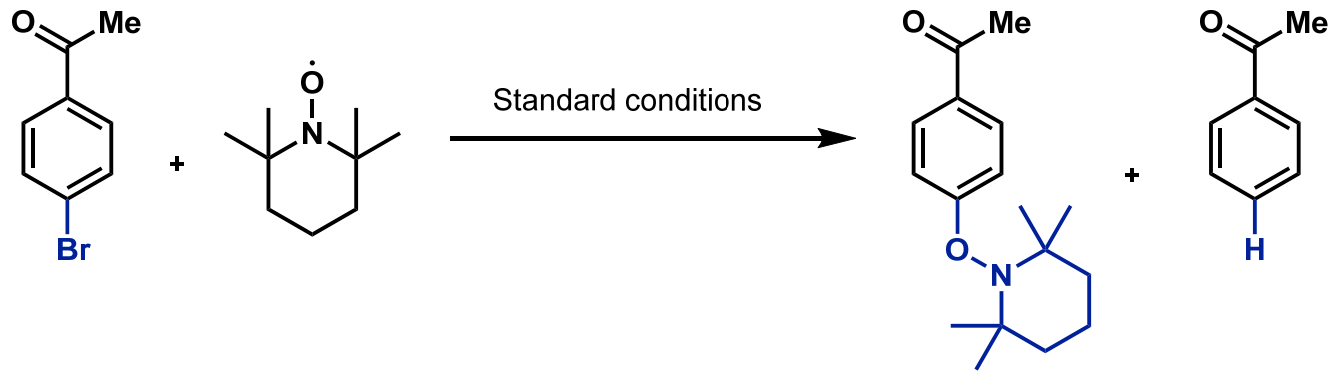

HRMS: calculated for $[M+H]^+$ $C_{17}H_{26}NO_2^+$ 276.1964; found 276.1959

Rationalization

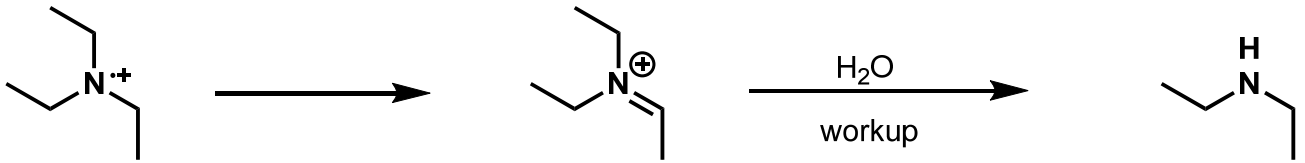

Diethylamine may come from the hydrogen abstraction of the triethylamine radical cation by aryl radical intermediate, affording the iminium intermediate which is hydrolyzed to diethylamine.

Ghosh, I.; Ghosh, T.; Bardagi, J. I.; König, B. *Science* **2014**, *346*, 725

Reductions driven by ConPET processes

Proposed mechanism

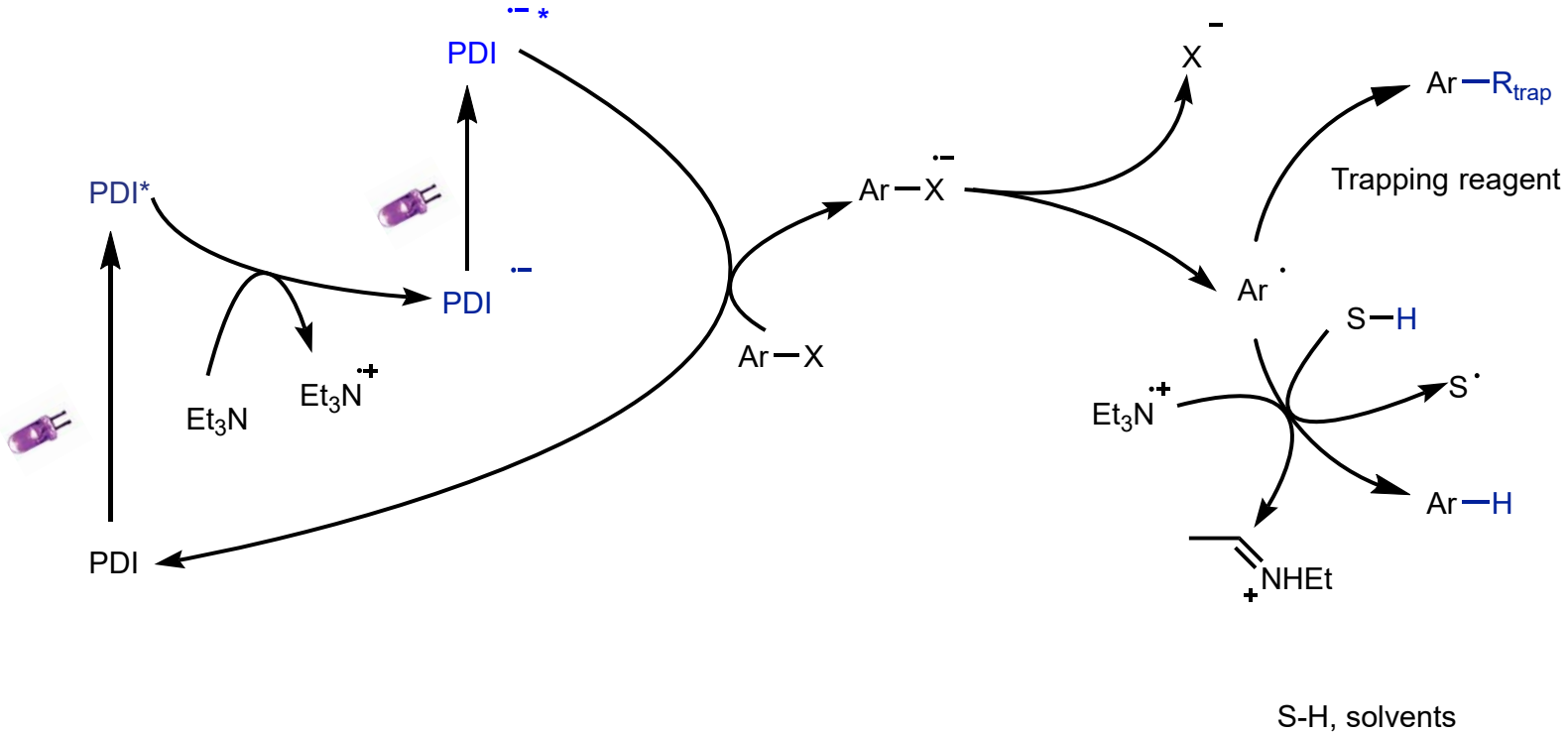

Ghosh, I.; Ghosh, T.; Bardagi, J. I.; König, B. *Science* **2014**, *346*, 725

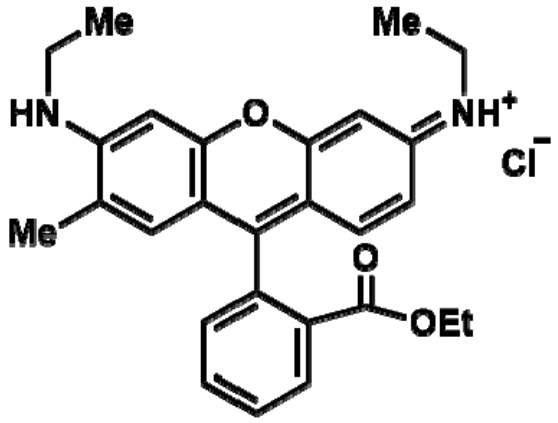

Rh-6G

König Burkhard
ACIE, **2016**, *55*, 7676

Reductions driven by ConPET processes

The spectrum of **Rh-6G**

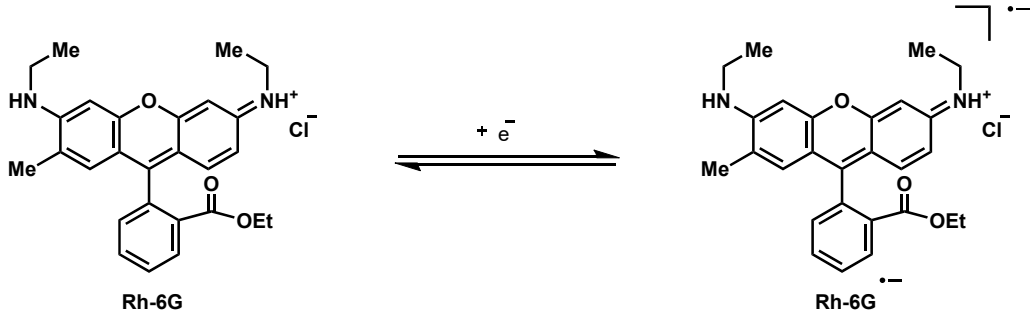

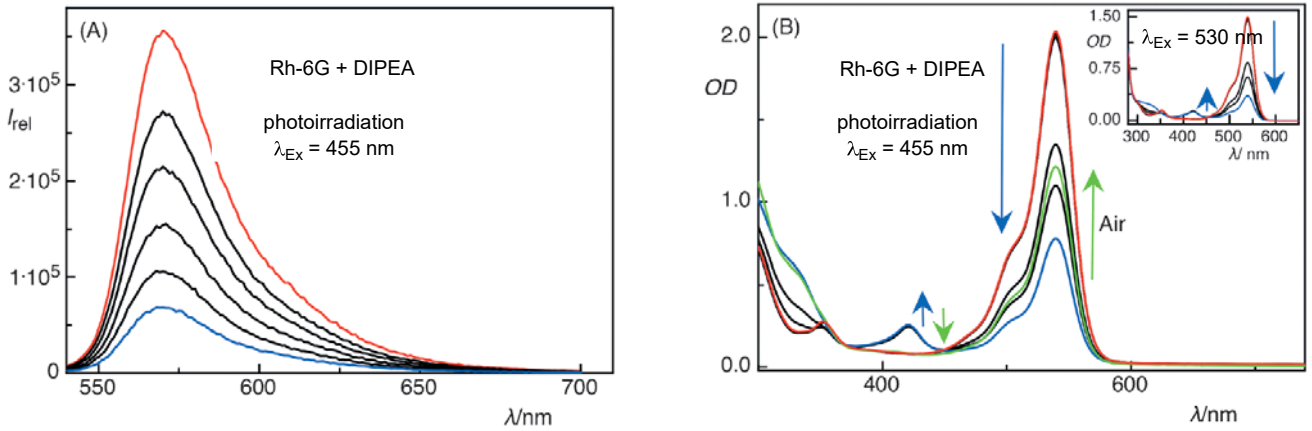

A: Changes in the fluorescence spectra of **Rh-6G** upon successive addition DIPEA in DMSO;

B: The absorption spectra of **Rh-6G** in the presence of DIPEA.

Rh-6G absorbs both in the green (530 nm) and blue (455 nm) regions, while **Rh-6G**$^{\bullet-}$ only absorbs in the blue (455 nm) region.

Ghosh, I.; König, B. *Angew. Chem. Int. Ed.*, **2016**, *55*, 7676

Reductions driven by ConPET processes

Controlled bond activation through light-color regulation of redox potentials

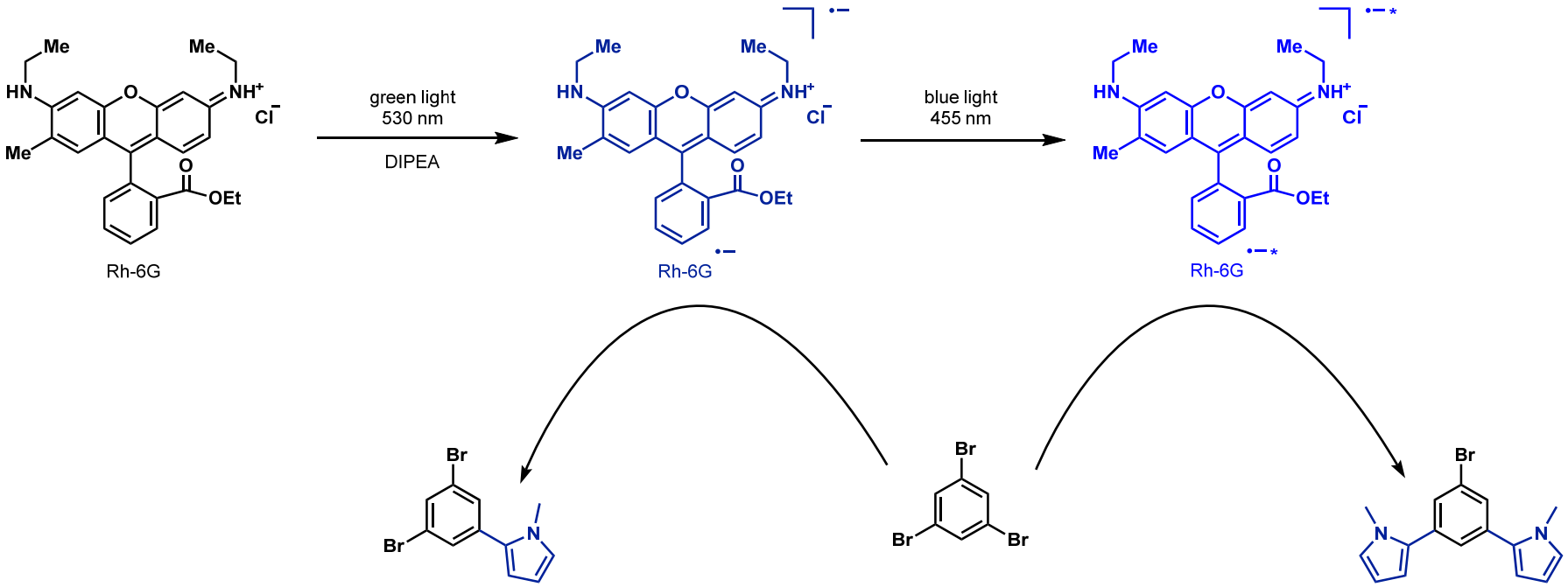

$E_{\text{Rh-6G/Rh-6G}^{\bullet-}} = -1.0$ V; $E_{\text{Rh-6G/Rh-6G}^{\bullet-*}} = -2.4$ V.

Ghosh, I.; König, B. *Angew. Chem. Int. Ed.*, **2016**, *55*, 7676

Reductions driven by ConPET processes

Mono- or di-substitutions

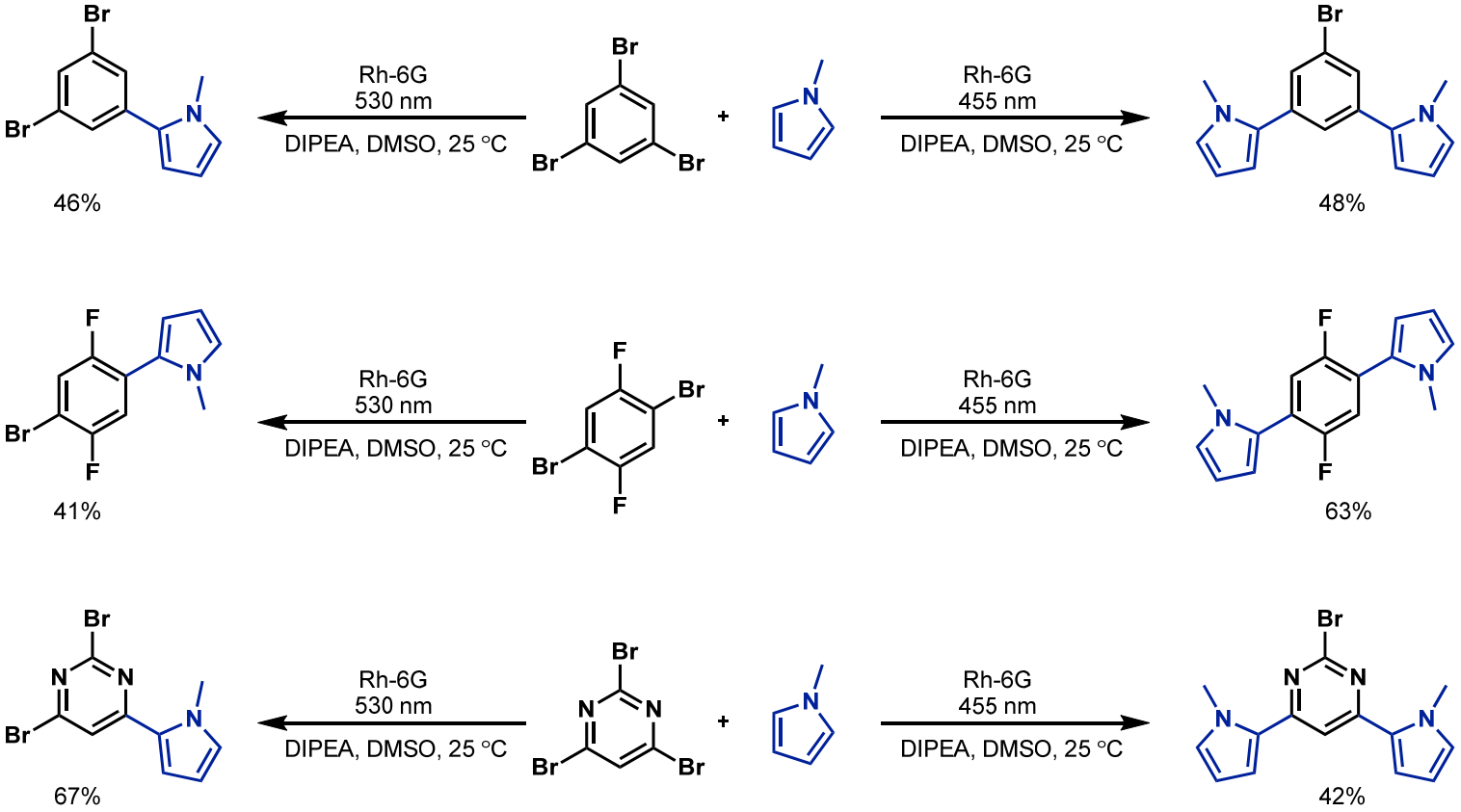

Ghosh, I.; König, B. *Angew. Chem. Int. Ed.*, **2016**, *55*, 7676

Reductions driven by ConPET processes

Proposed mechanism

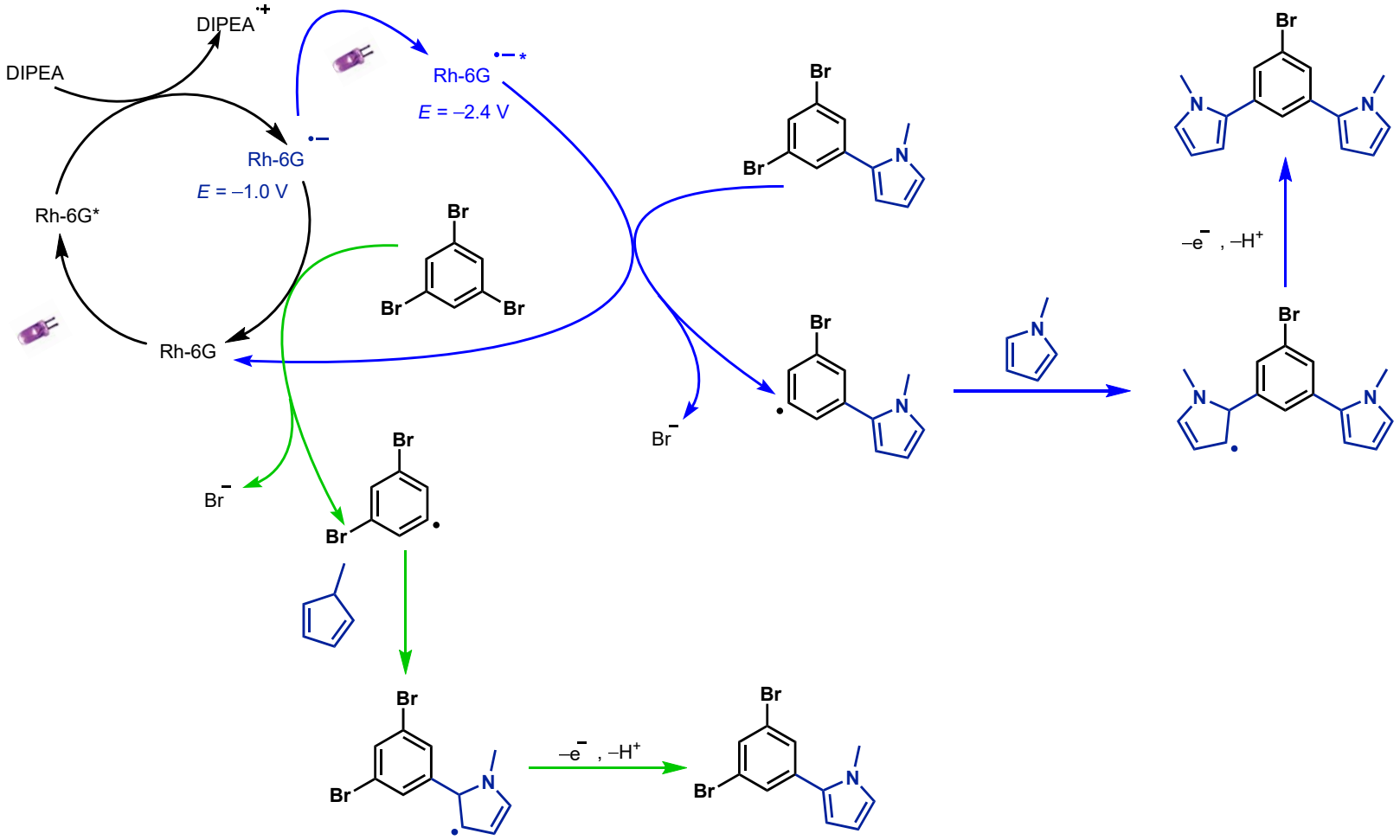

Ghosh, I.; König, B. *Angew. Chem. Int. Ed.*, **2016**, *55*, 7676

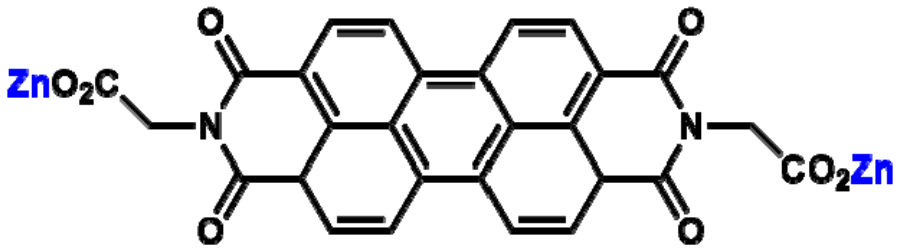

Zn-PDI

Duan Chunying
JACS, **2016**, *138*, 3958

Reductions driven by ConPET processes

Synthesis of **Zn-PDI** (a heterogeneous photocatalyst)

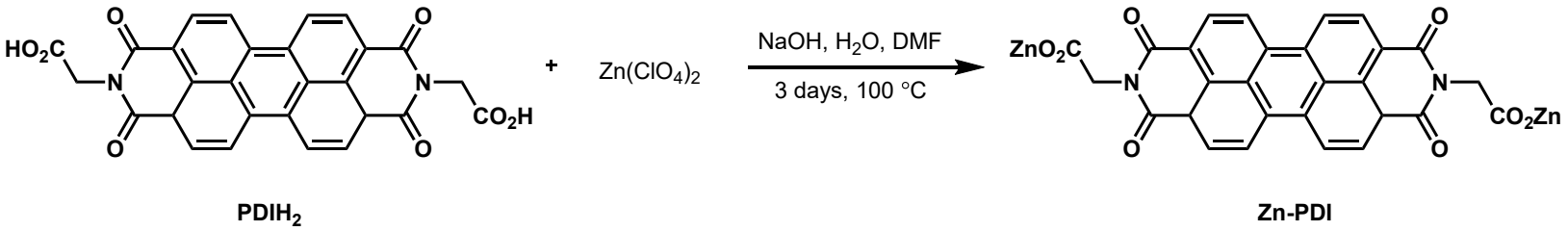

$PDIH_2$

Zn-PDI

44% yield through filtration

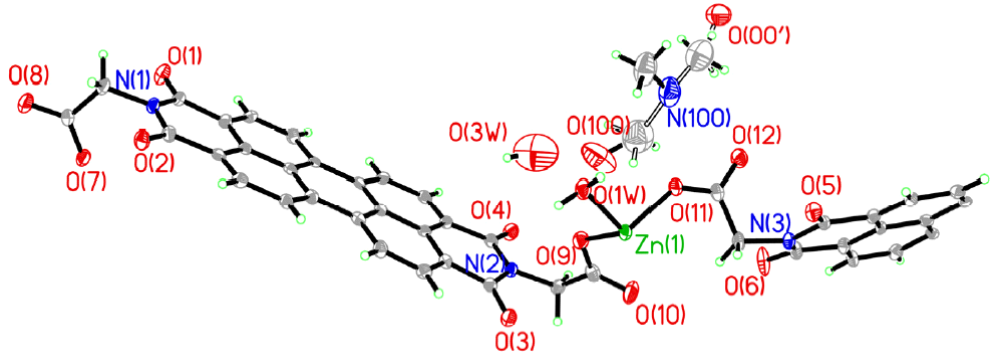

Single crystal X-ray crystallography of **Zn-PDI**

Duan, C.Y. et al. *J. Am. Chem. Soc.* **2016**, *138*, 39588

Reductions driven by ConPET processes

Structural features of **Zn-PDI**

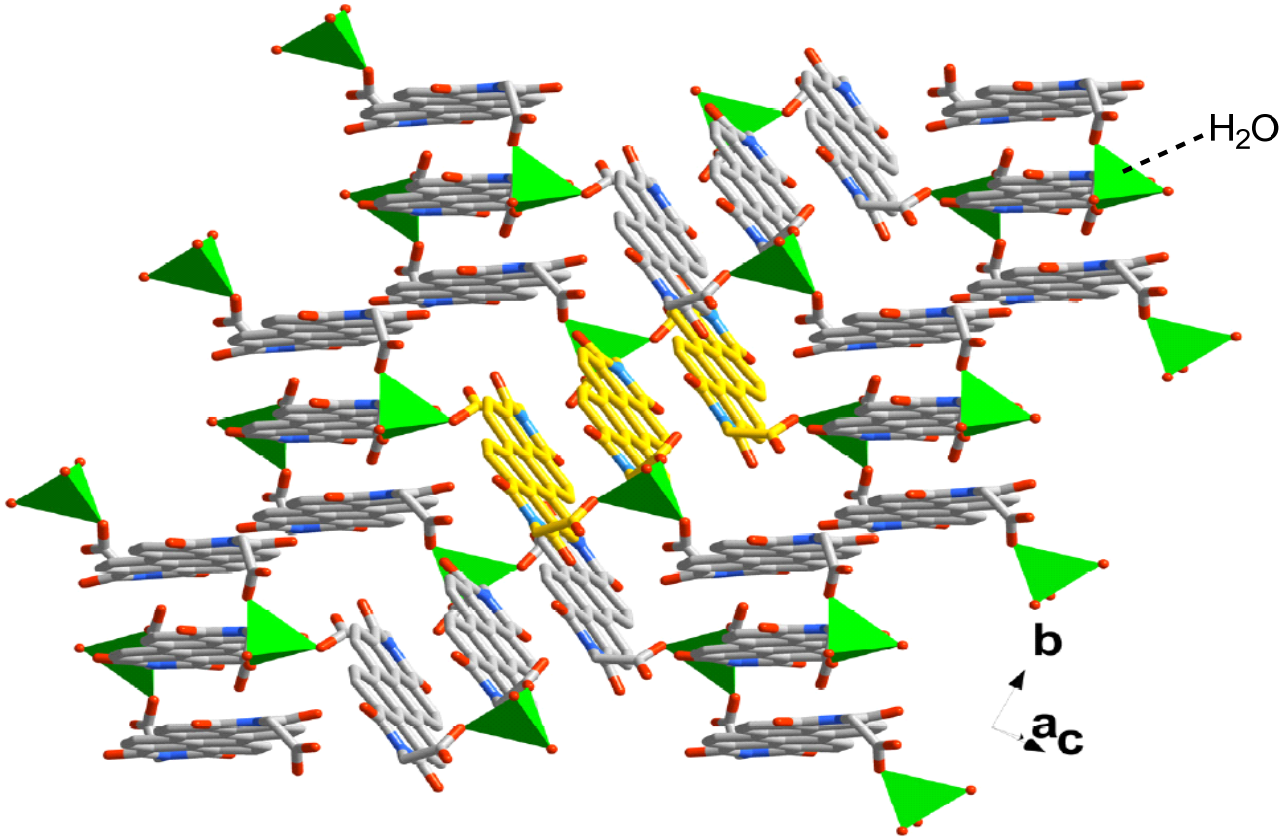

Ball-and-stick representation of **PDI** fragments in 2D layer

Each zinc ion was coordinated by three carboxylic groups from three deprotonated **PDI** ligands and one water molecule. Because of strong π···π interactions between **PDIs**, the geometry of **ZnPDI** is a distorted tetrahedron.

Duan, C.Y. et al. *J. Am. Chem. Soc.* **2016**, *138*, 39588

Reductions driven by ConPET processes

The spectrum of **Zn-PDI**

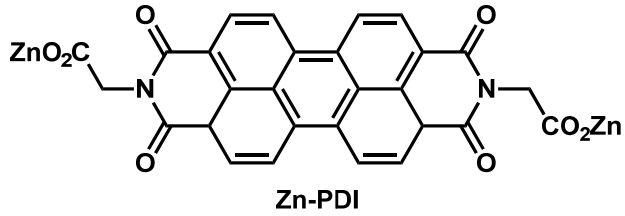

Zn-PDI

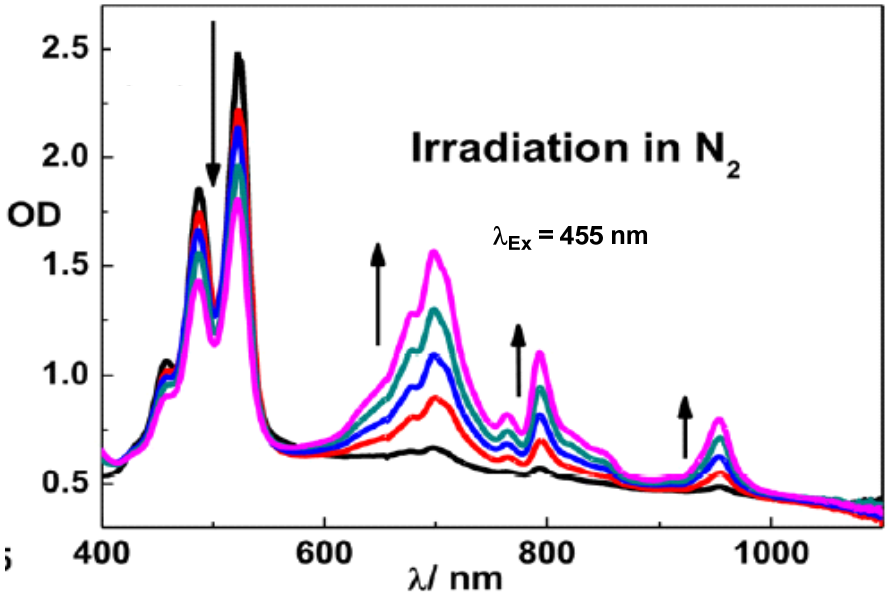

The absorption spectra of **Zn-PDI** in the presence of Et_3N.

The absorption spectrum of **Zn-PDI** is similar with **PDI** reported by König B. in 2014.

Duan, C.Y. et al. *J. Am. Chem. Soc.* **2016**, *138*, 39588

Reductions driven by ConPET processes

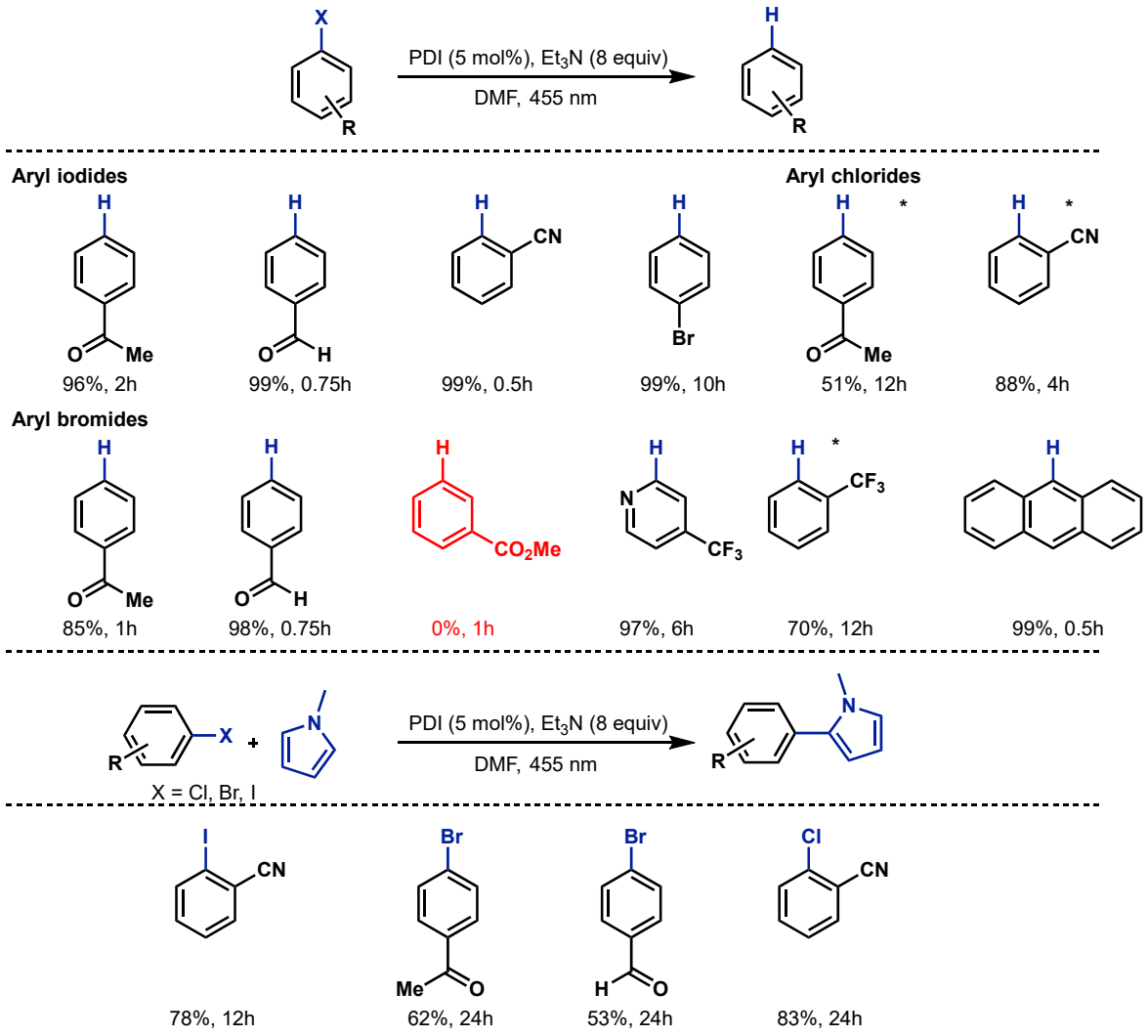

* 10 mol% catalyst was employed.

Duan, C.Y. et al. *J. Am. Chem. Soc.* **2016**, *138*, 39588

Reductions driven by ConPET processes

Proposed mechanism

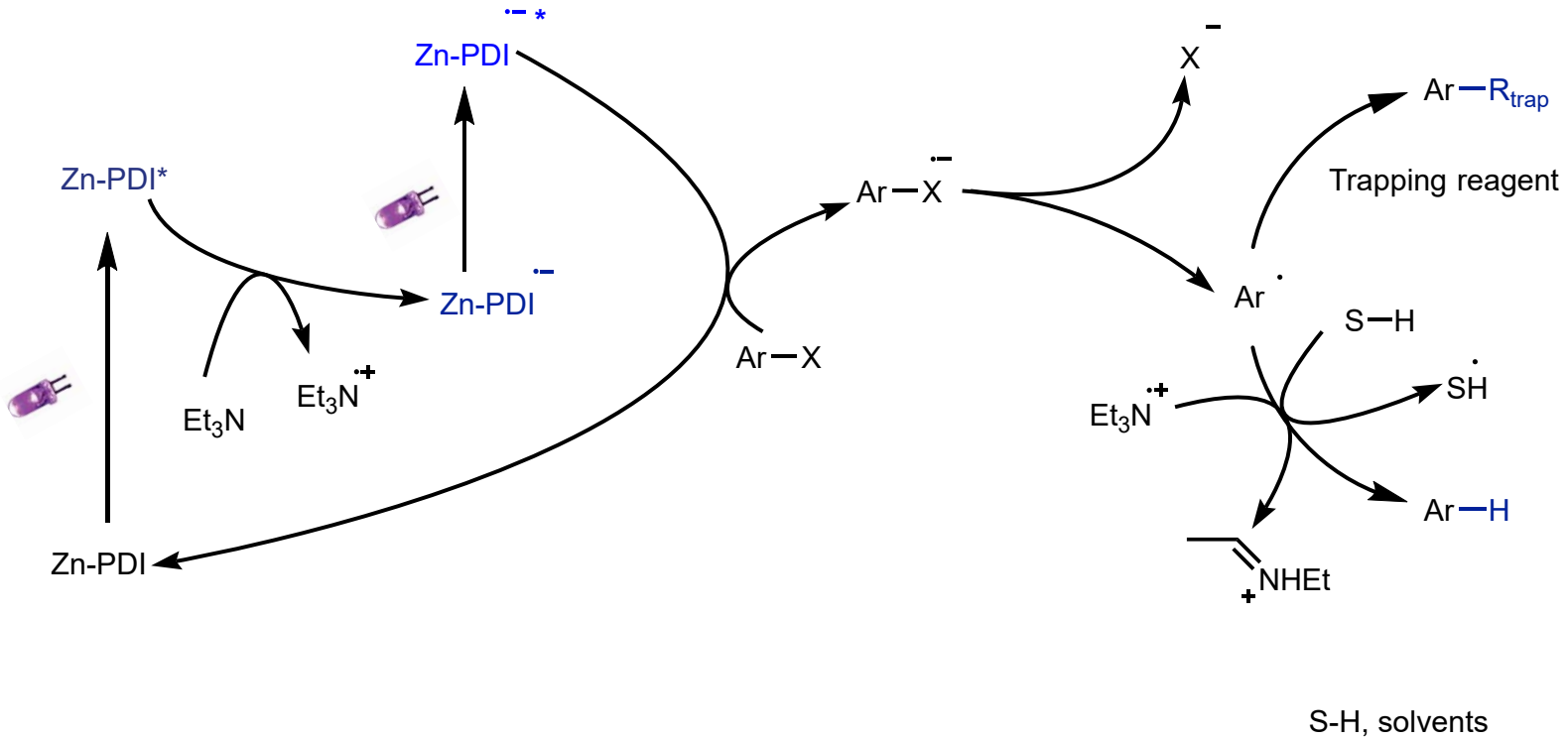

The mechanism of the reaction is the same as that proposed by König B. in 2014.

Duan, C.Y. et al. *J. Am. Chem. Soc.* **2016**, *138*, 39588

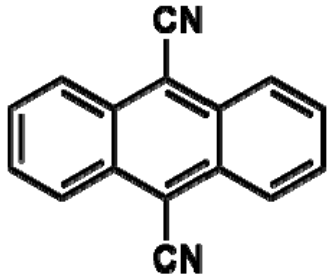

dicyanoanthracene (**DCA**)

Pérez-Ruiz Raul
Chem. Eur. J., **2018**, *24*, 105

Reductions driven by ConPET processes

The spectrum of **DCA**

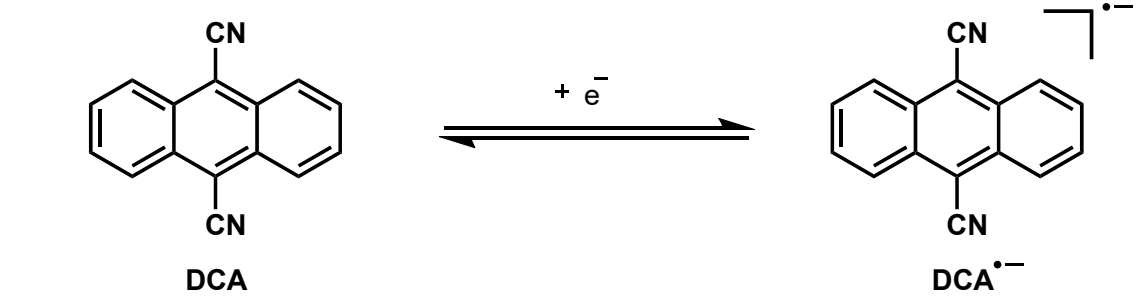

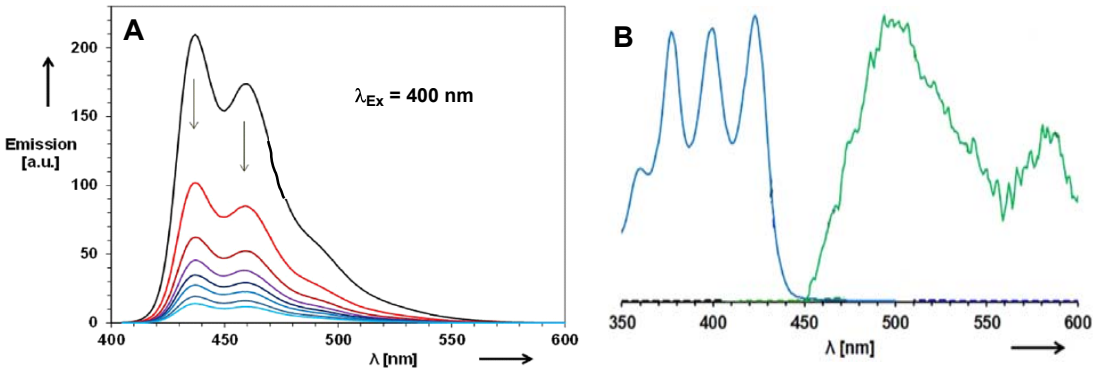

A: Changes in the fluorescence spectra of **DCA** upon successive addition DIPEA in DMSO;

B: The absorption spectra of **DCA** (blue line) and **DCA**$^{\bullet-}$ absorption (green line).

Although absorption wavelengths are different, they both locate in the visible light range.
The reduction potential of excited **DCA**$^{\bullet-}$ is −2.5 V, which is sufficient to reduce aryl bromides.

Rérez-Ruiz, R. et al. *Chem. Eur. J.* **2018**, 105

Reductions driven by ConPET processes

Control experiments

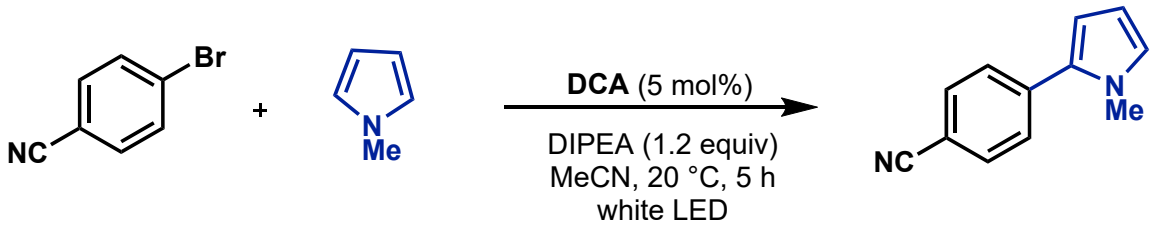

Entry	Reaction condition	Time (h)	Yield (%)
1	No change	5	82
2	without DIPEA	5	0
3	without photocatalyst	5	0
4	Dark	5	0
5	455 nm or 525 nm, N_2	5	< 4

Rérez-Ruiz, R. et al. *Chem. Eur. J.* **2018**, 105

Reductions driven by ConPET processes

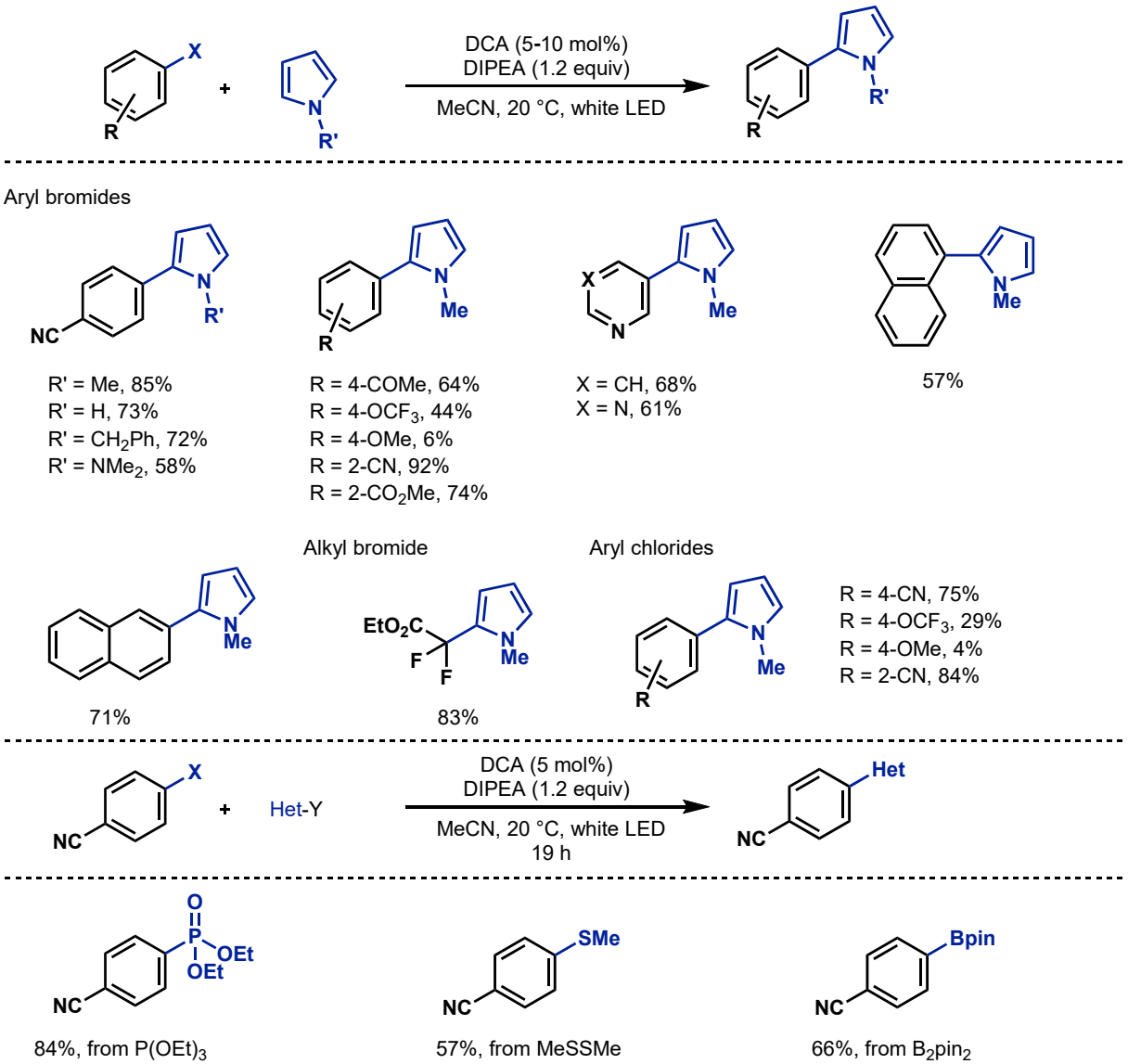

Rérez-Ruiz, R. et al. *Chem. Eur. J.* **2018**, 105

Reductions driven by ConPET processes

Proposed mechanism

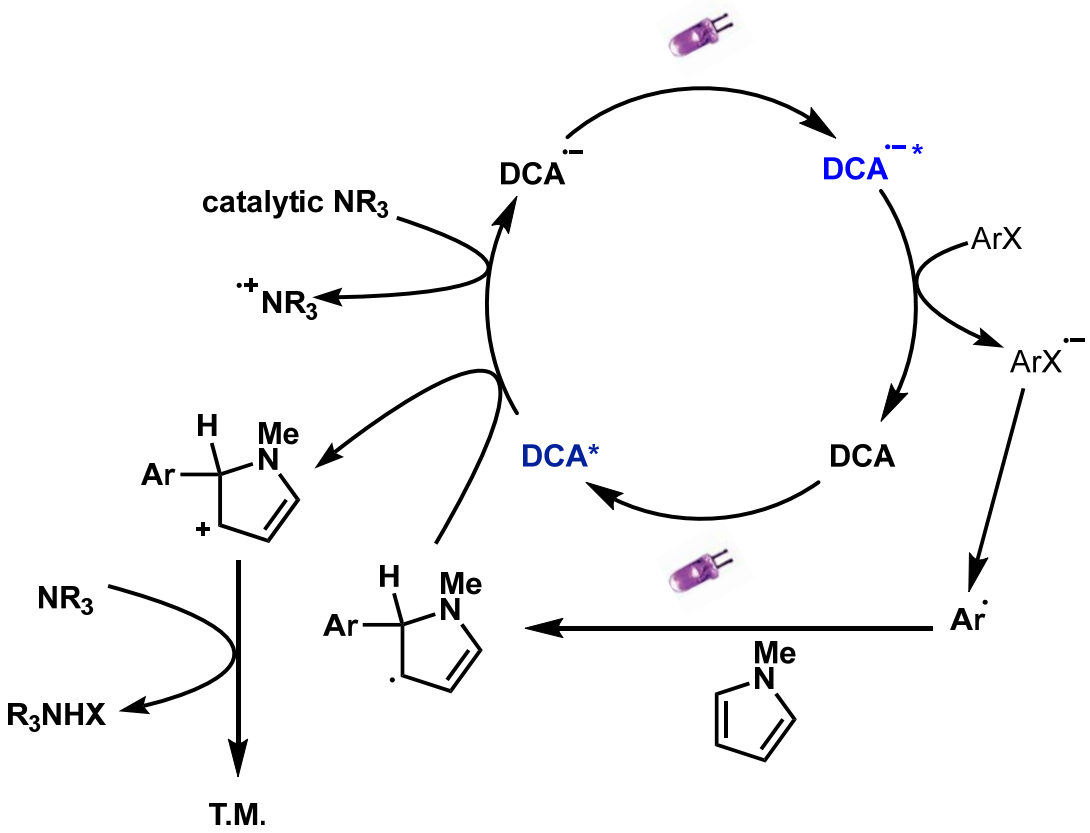

Rérez-Ruiz, R. et al. *Chem. Eur. J.* **2018**, 105

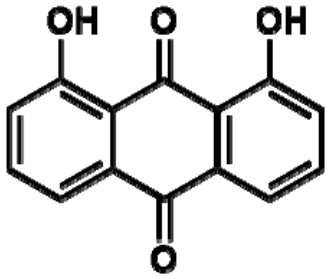

dihydroxyanthraquinone (**Aq-OH**)

König Burkhard
Eur. J. Org. Chem., **2018**, 34

Reductions driven by ConPET processes

The spectra of **Aq-OH**

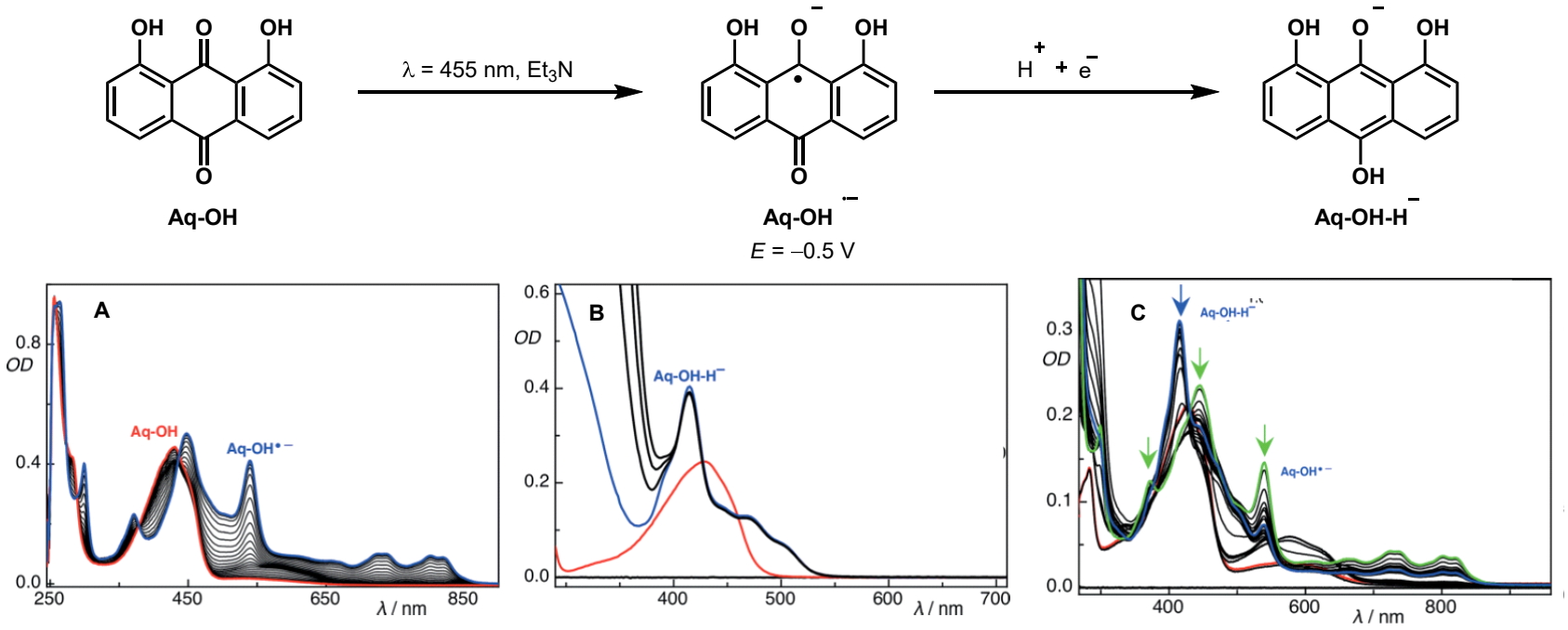

A: Spectroelectrochemistry of Aq-OH in DMF; **B**: The absorption spectrum of **Aq-OH-H⁻** (Formation of **Aq-OH-H⁻** in the presence of $Na_2S_2O_4$); **C**: Changes to the absorption spectra of **Aq-OH** upon photoirradiation (λ_{Ex} = 455 ± 15 nm) in the presence of Et_3N under nitrogen in DMF.

König, B. et al. *Eur. J. Org. Chem.* **2018**, 34

Reductions driven by ConPET processes

Dehalogenation

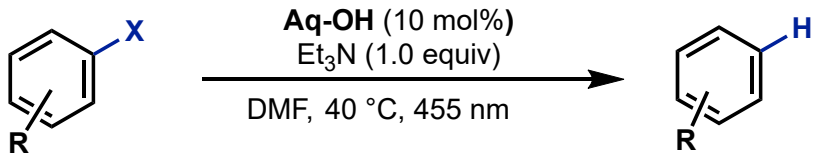

Aryl bromides

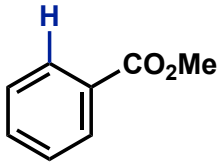

74%

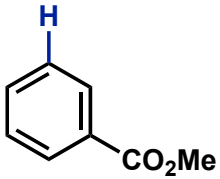

87%

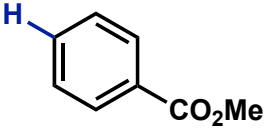

51%

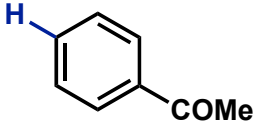

80%

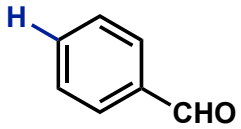

85%

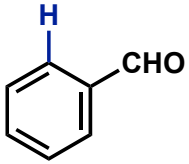

56%

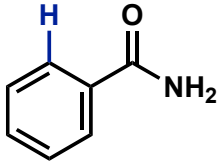

40%

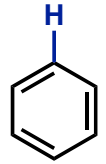

4%

Aryl iodides

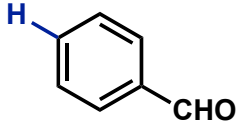

60%

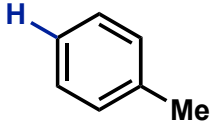

27%

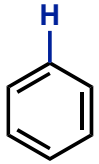

25%

König B. et al. *Eur. J. Org. Chem.*, **2018**, 34

Reductions driven by ConPET processes

Proposed mechanism

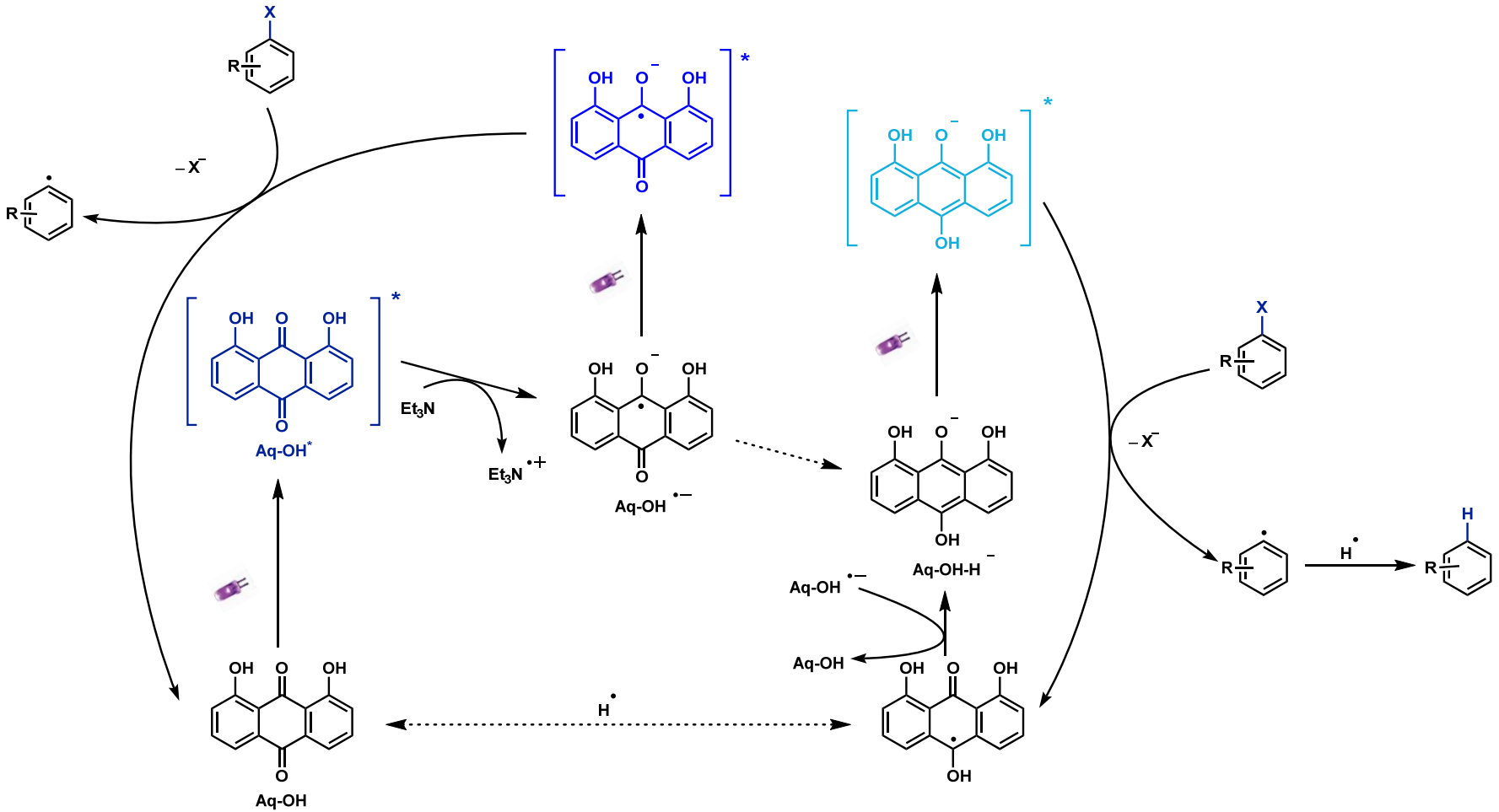

König B. et al. *Eur. J. Org. Chem.*, **2018**, 34

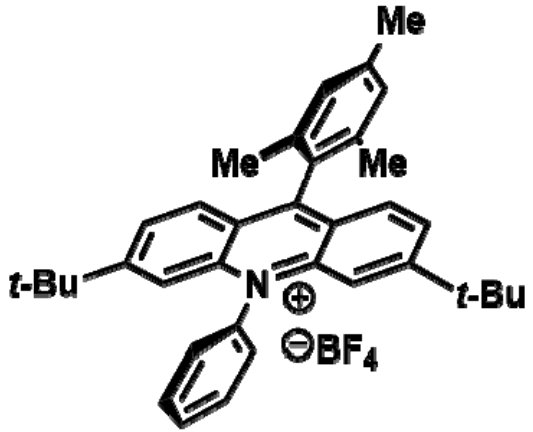

Mes-Acr-BF_4

Nicewicz David A.
Nature **2020**, 76

Reductions driven by ConPET processes

The property of **Mes-Acr-BF_4**

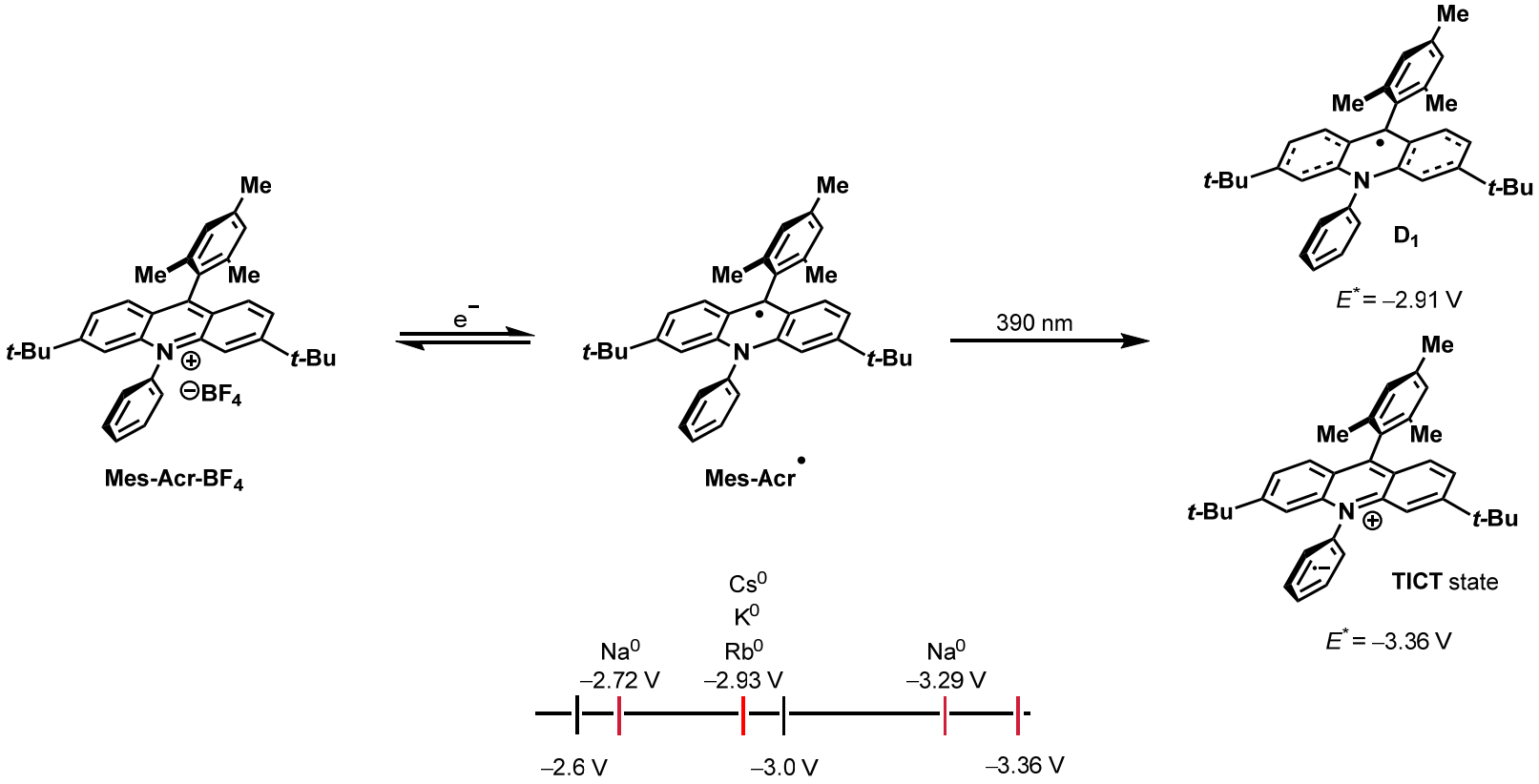

There are two main excited states, assigned as lower energy doublet (**D_1**) and a higher energy twisted intramolecular charge transfer (**TICT**) state.

Nicewicz, D. A. et al. *Nature* **2020**, *580*, 76

Reductions driven by ConPET processes

The molecular orbtials of **Mes-Acr•**

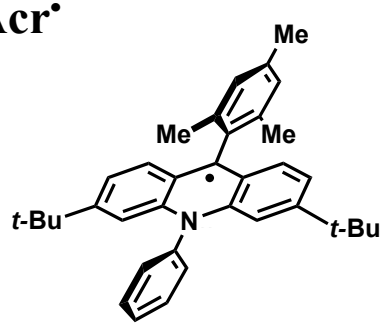

Mes-Acr•

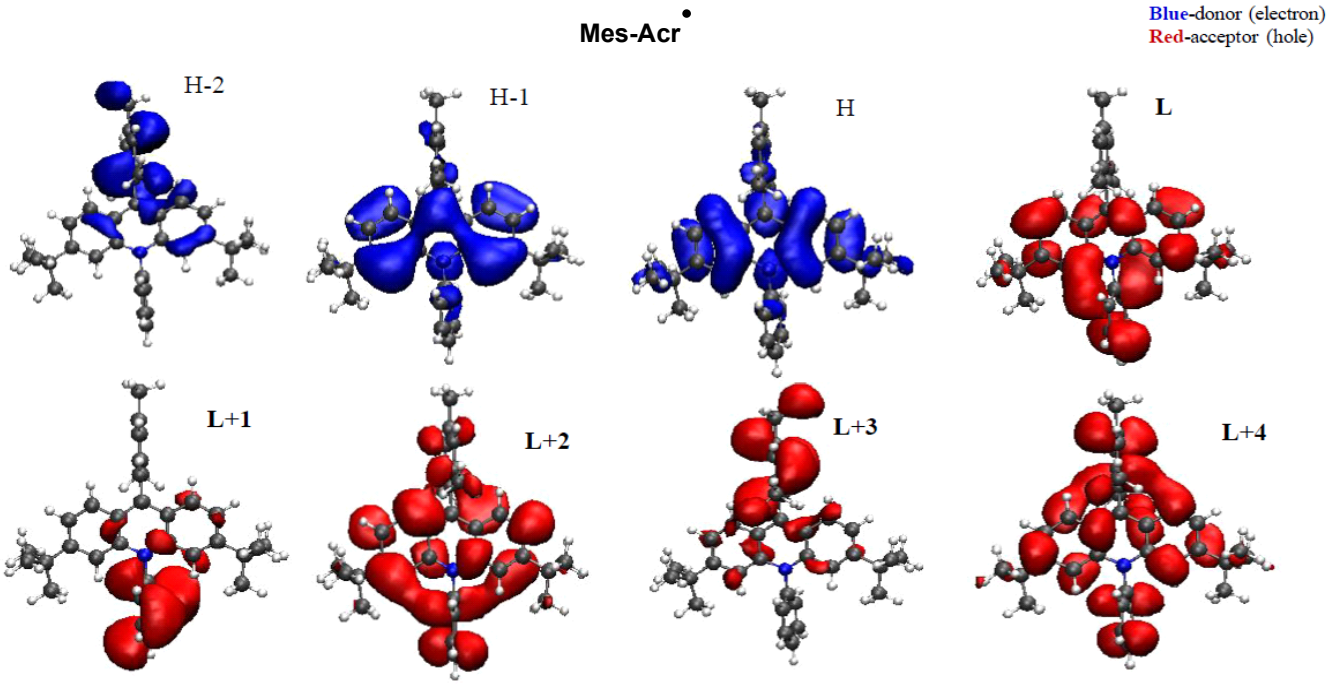

Nicewicz, D. A. et al. *Nature* **2020**, *580*, 76

Reductions driven by ConPET processes

TICT state of **Mes-Acr•**

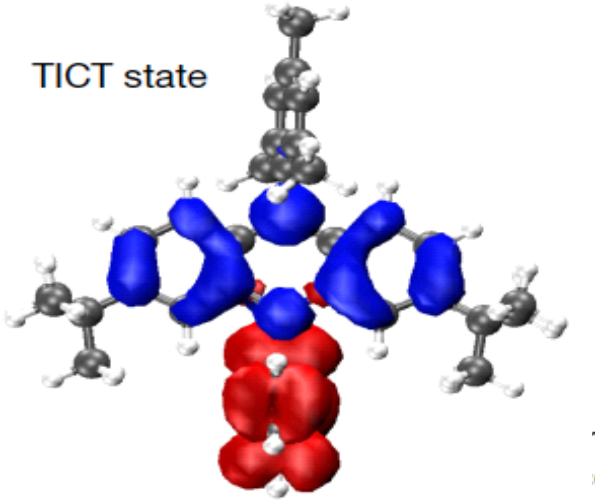

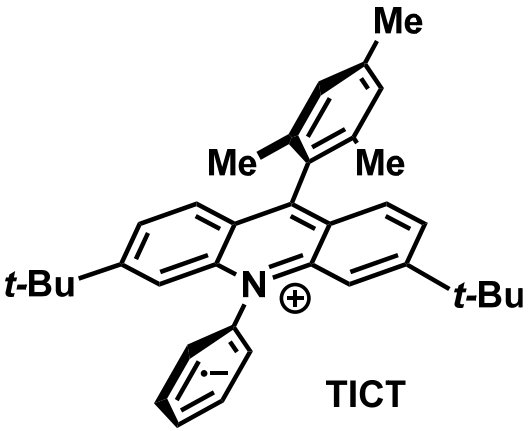

E^*_{ox} = –3.36 V

If the electron is excited from SOMO to LUMO+1, the process is equivalent to an intramolecular charge transfer, where electron is transferred from acridine to *N*-Phenyl ring.

Nicewicz, D. A. et al. *Nature* **2020**, *580*, 76

Reductions driven by ConPET processes

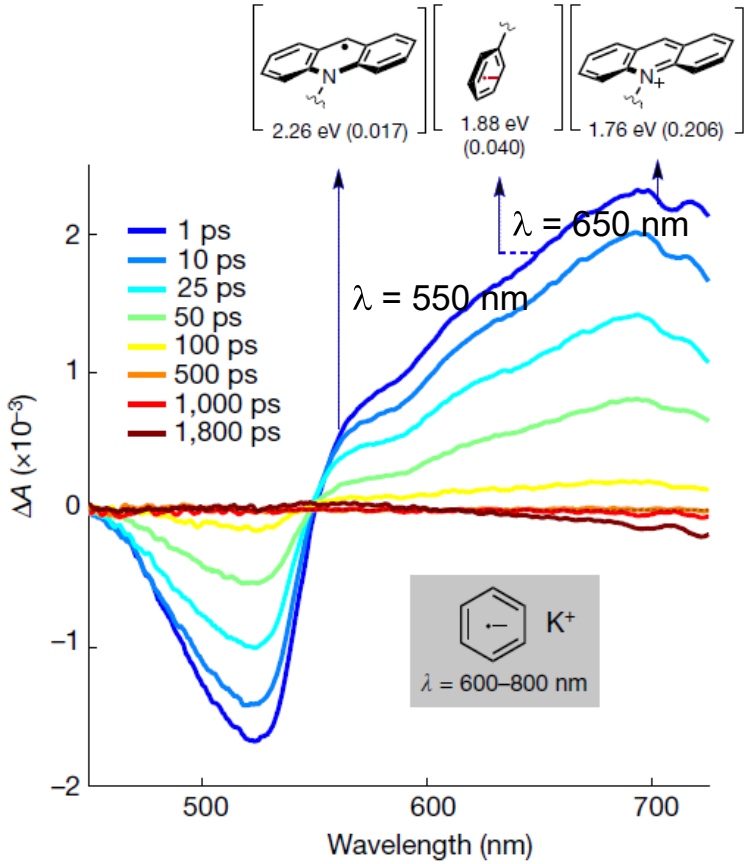

Transient absorption spectra of **Mes-Acr•**

Exited-state absorbance resonances with maxima at 550 and 650 nm are observed, which match the absorbance profile of aromatic radical anion. This indicates **Mes-Acr•**, in its excited state, acts as if it were a radical anion.

Nicewicz, D. A. et al. *Nature* **2020**, *580*, 76

Reductions driven by ConPET processes

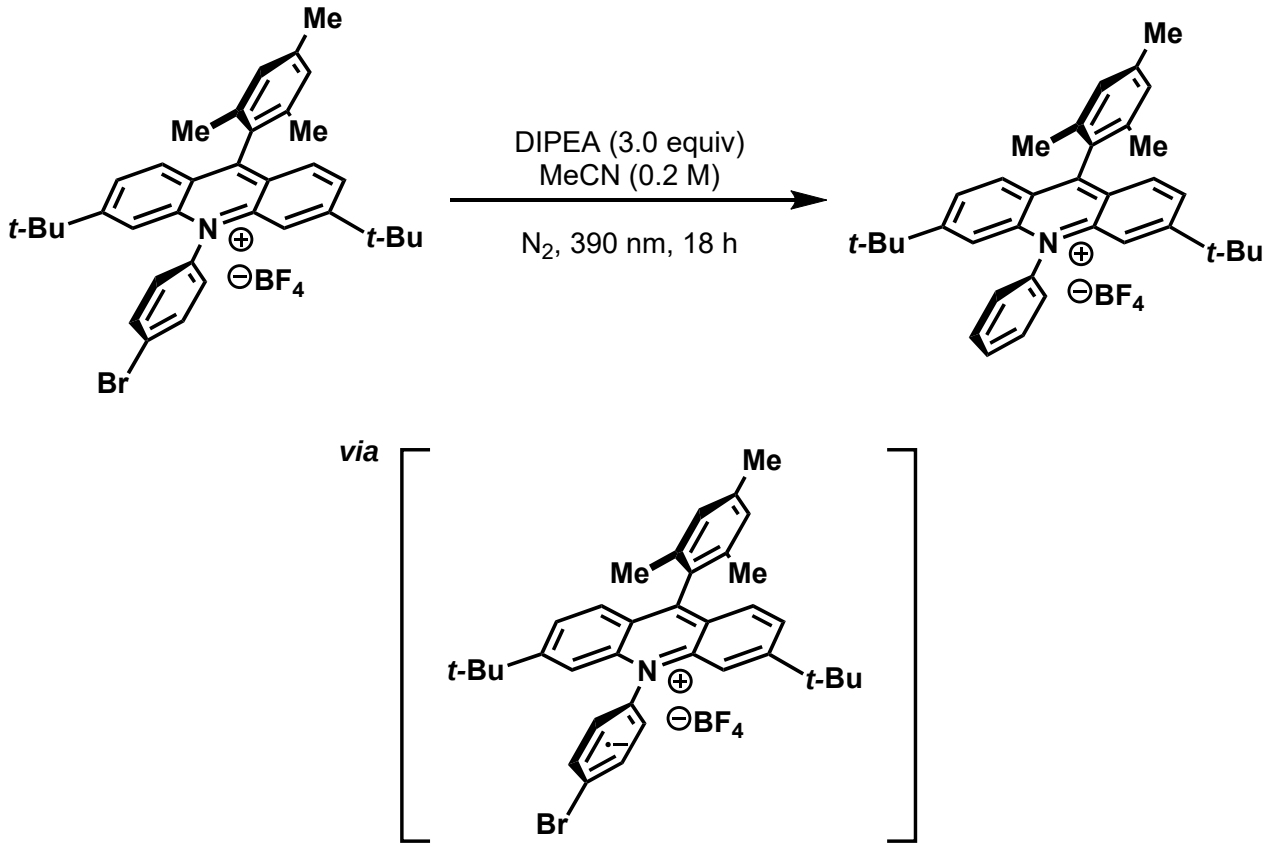

This experiment is indicative of the formation of radical anion localized on the *N*-phenyl ring during excitation.

Nicewicz, D. A. et al. *Nature* **2020**, *580*, 76

Reductions driven by ConPET processes

Dehalogenation

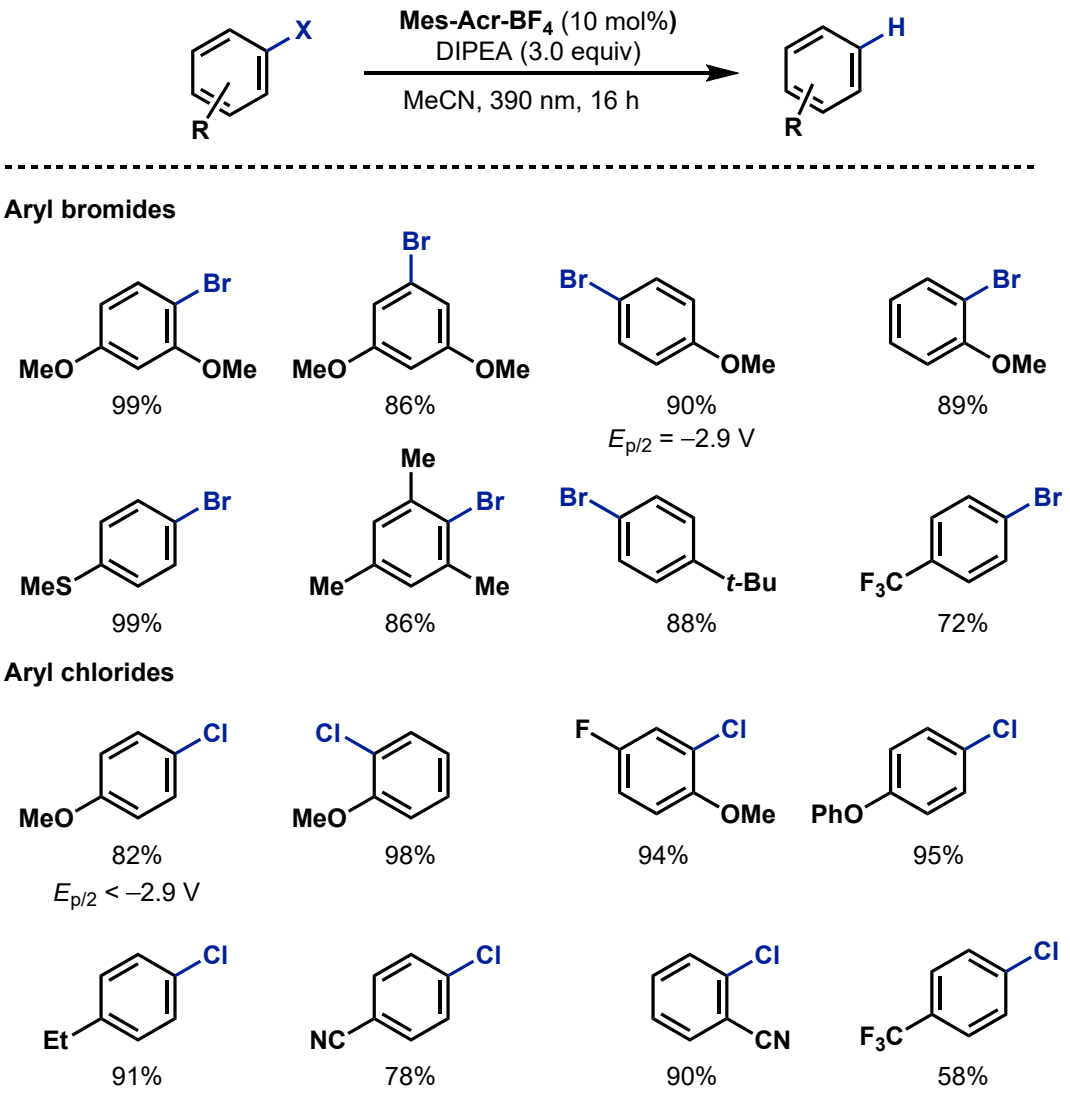

Nicewicz, D. A. et al. *Nature* **2020**, *580*, 76

Reductions driven by ConPET processes

Detosylation

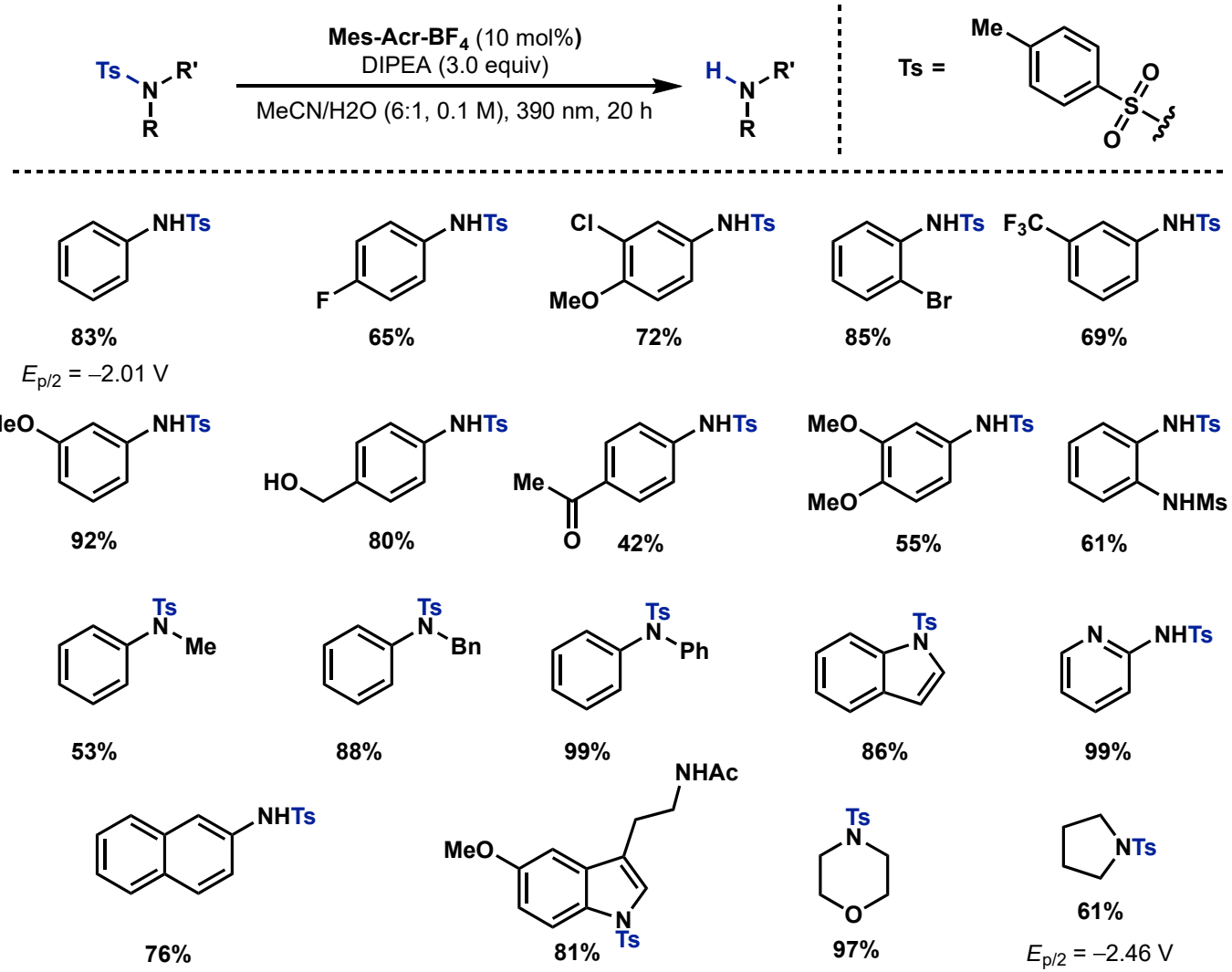

Nicewicz, D. A. et al. *Nature* **2020**, *580*, 76

Reductions driven by ConPET processes

Proposed mechanism

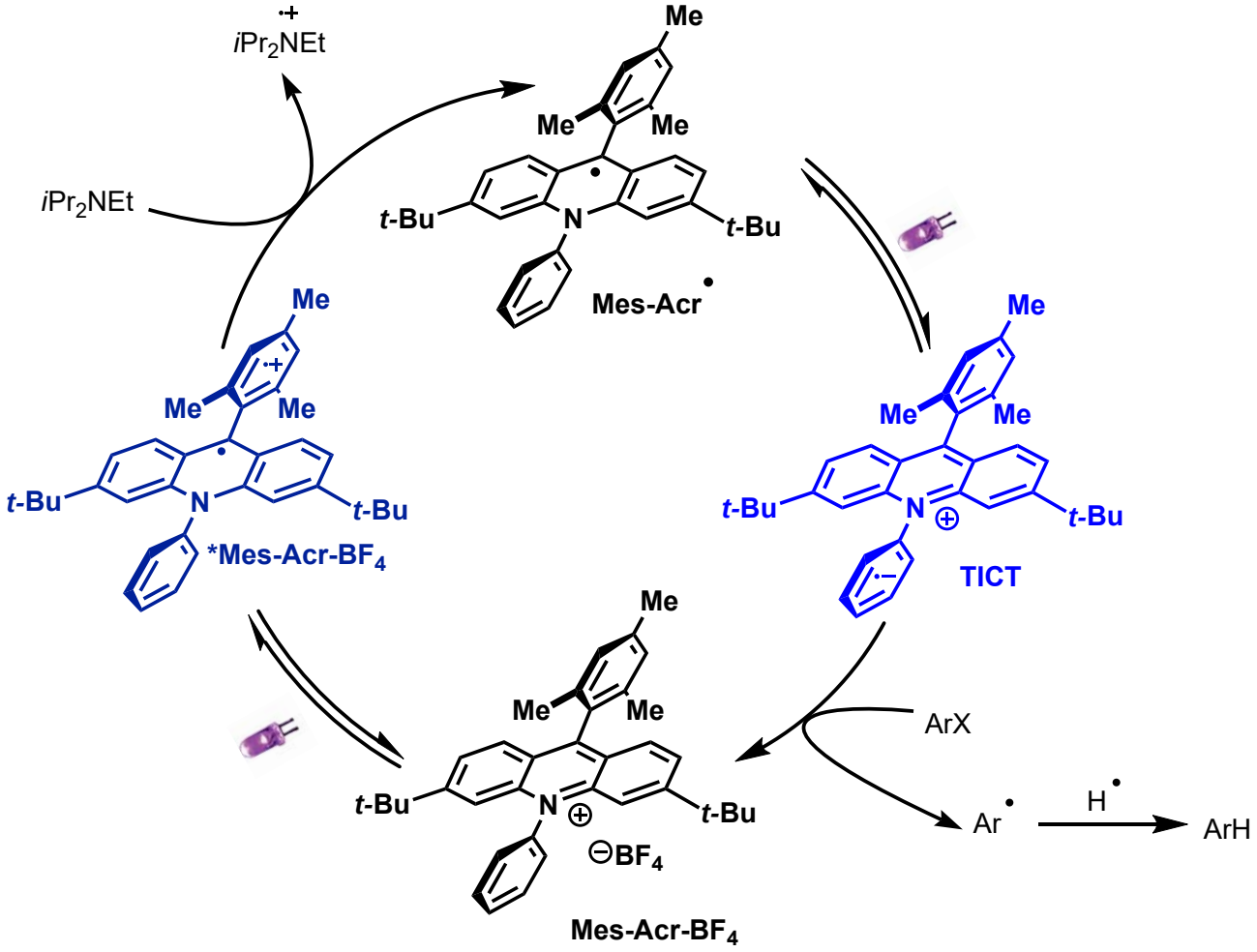

Nicewicz, D. A. et al. *Nature* **2020**, *580*, 76

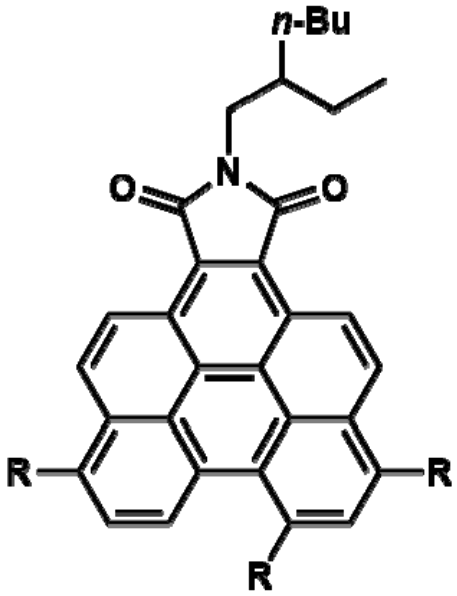

Benzo[ghi]perylene (**BPI**)

Miyake Garret M.
JACS, **2020**, *142*, 13573

Reductions driven by ConPET processes

The property of BPI

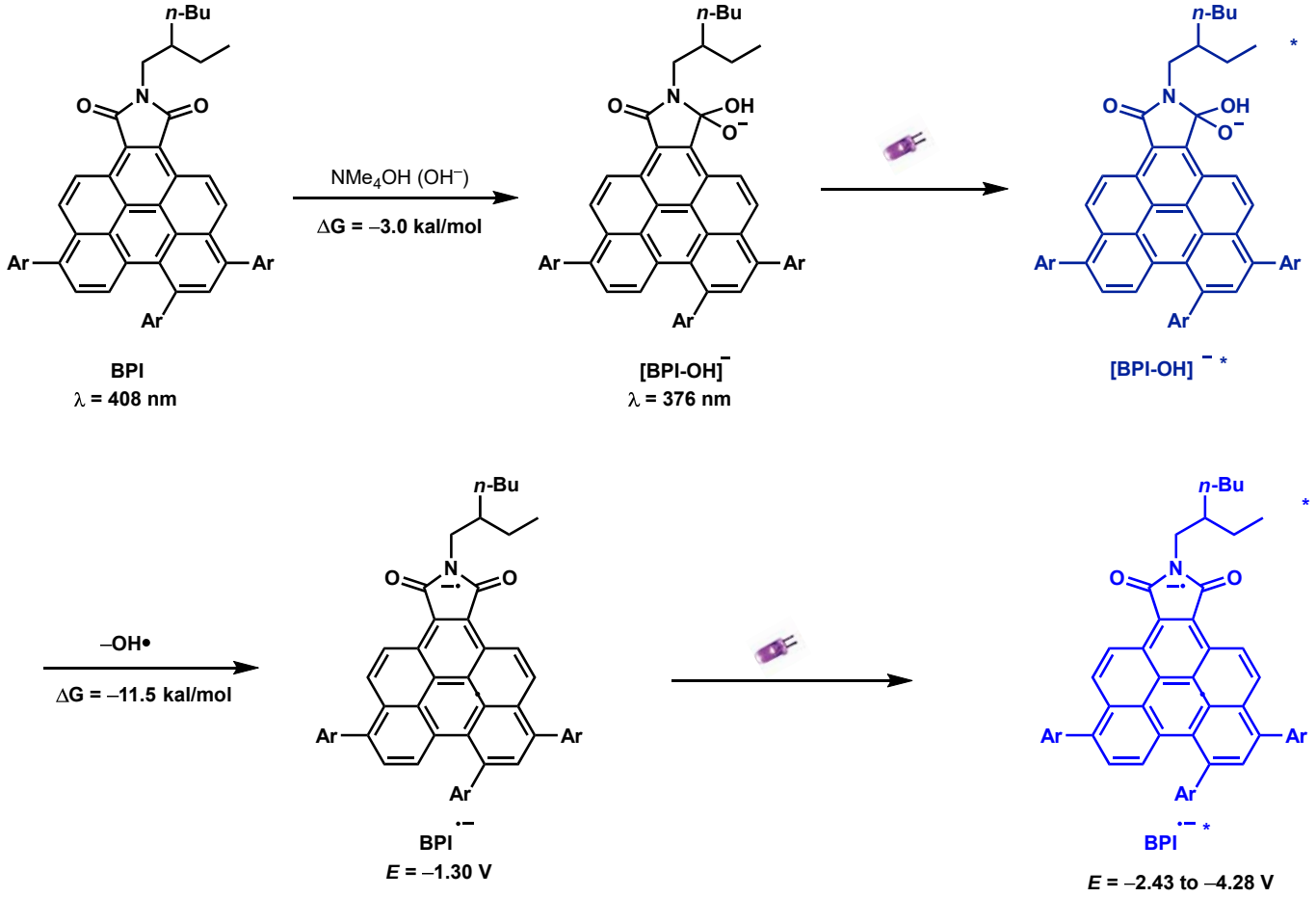

PC$^{\bullet-}$ can be photoexcited, where **the first six excited states** are predicted from TDDFT calculations. Ar = 4-OMePh.

Miyake, G. M. et al. *J. Am. Chem. Soc.* **2020**, *142*, 13573

Reductions driven by ConPET processes

Proposed generation of solvated electron by $PC^{\bullet -}$*

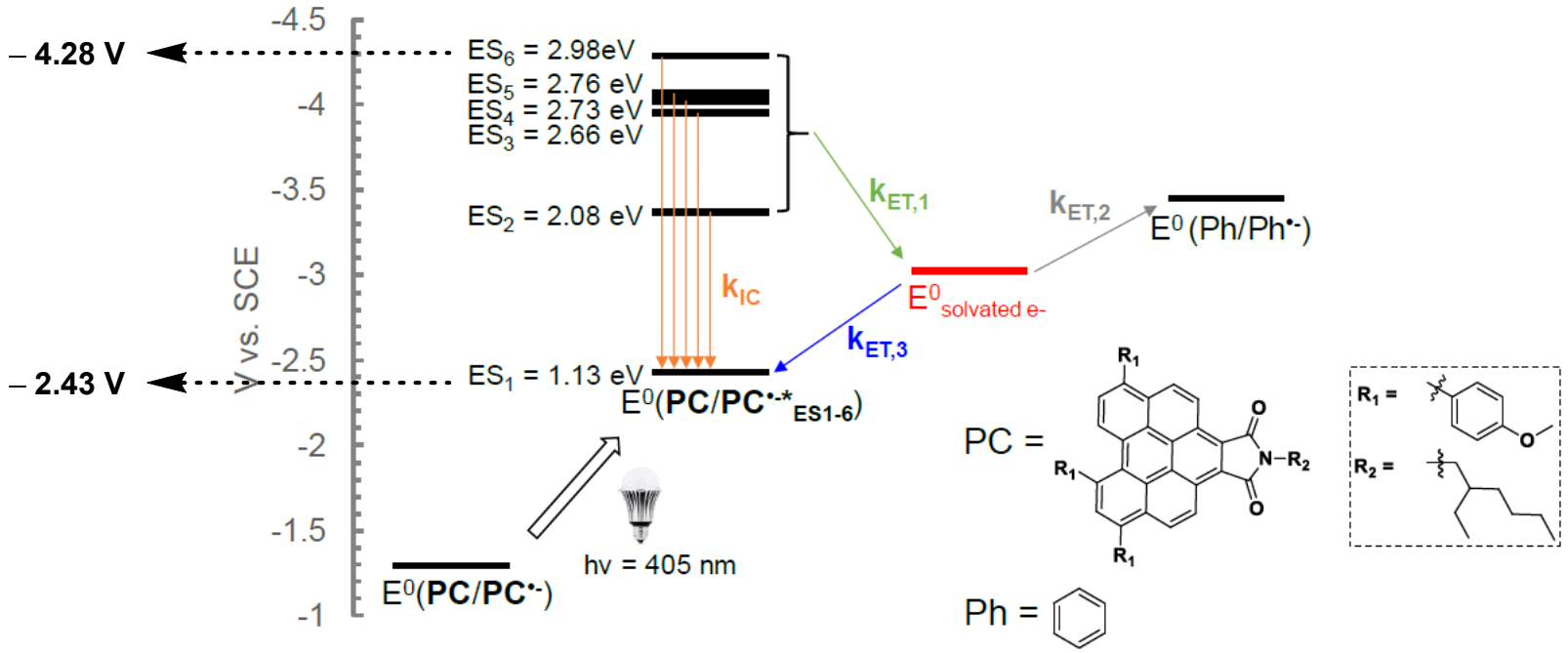

$k_{ET,1}$: ionization of $PC^{\bullet -}$* by an electron transfer to the solvent;

$k_{ET,2}$: electron transfer from the solvated electron to an aromatic substrate;

$k_{ET,3}$: back electron transfer to the lowest excited state of **$PC^{\bullet -}$***;

k_{IC}: the internal conversion process.

Miyake, G. M. et al. *J. Am. Chem. Soc.* **2020**, *142*, 13573

Reductions driven by ConPET processes

Birch reduction

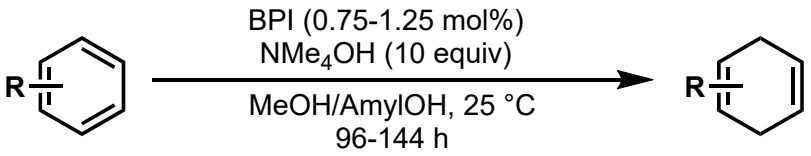

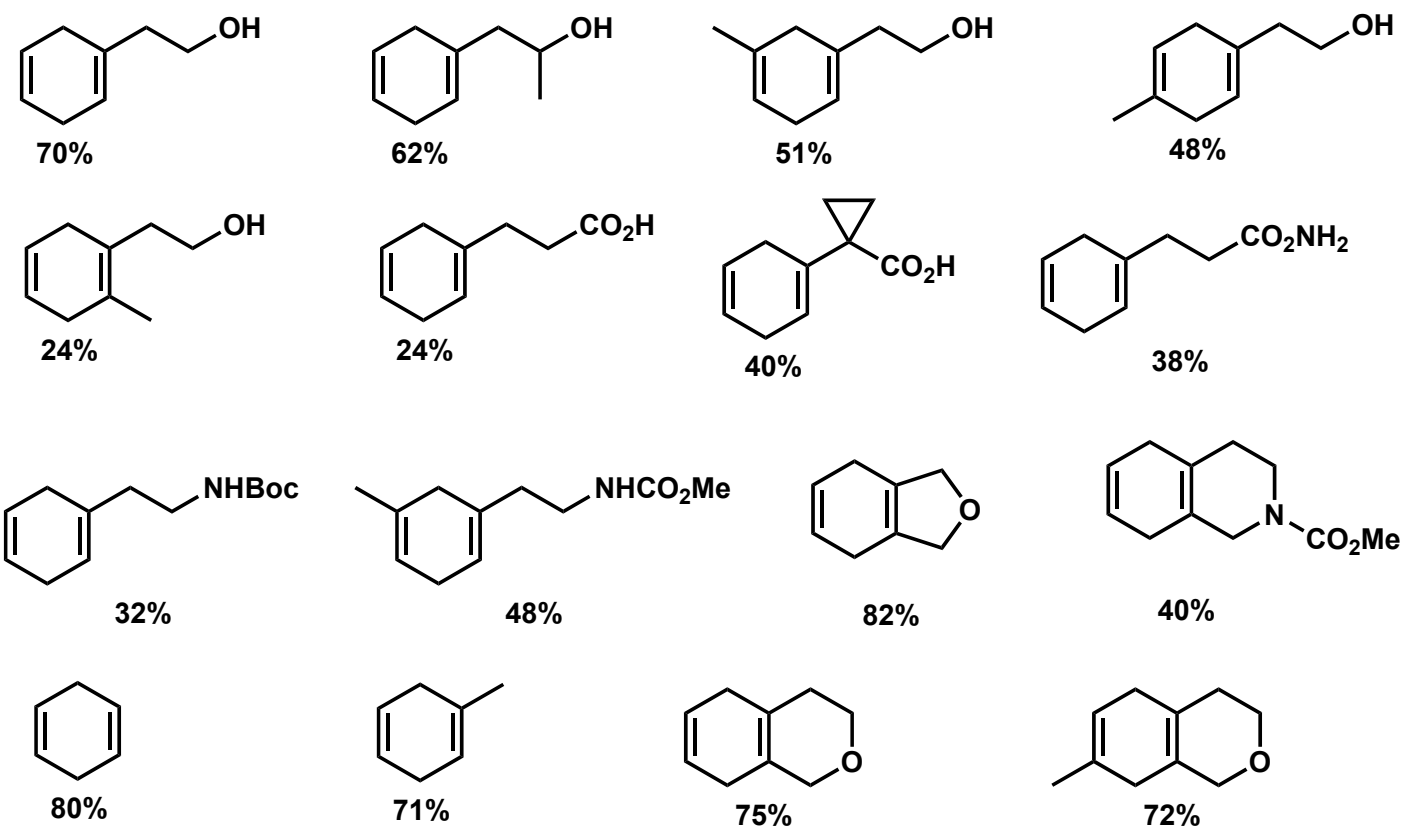

Miyake, G. M. et al. *J. Am. Chem. Soc.* **2020**, *142*, 13573

Content

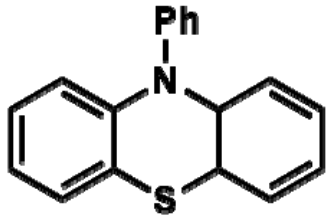

N-phenylphenothiazine (**PTH**)

ChemCatChem ***2018***, *10*, 2955;
ACIE, **2020**, 59, 300;
JACS, **2021**, *143*, 4125

Oxidations driven by ConPET processes

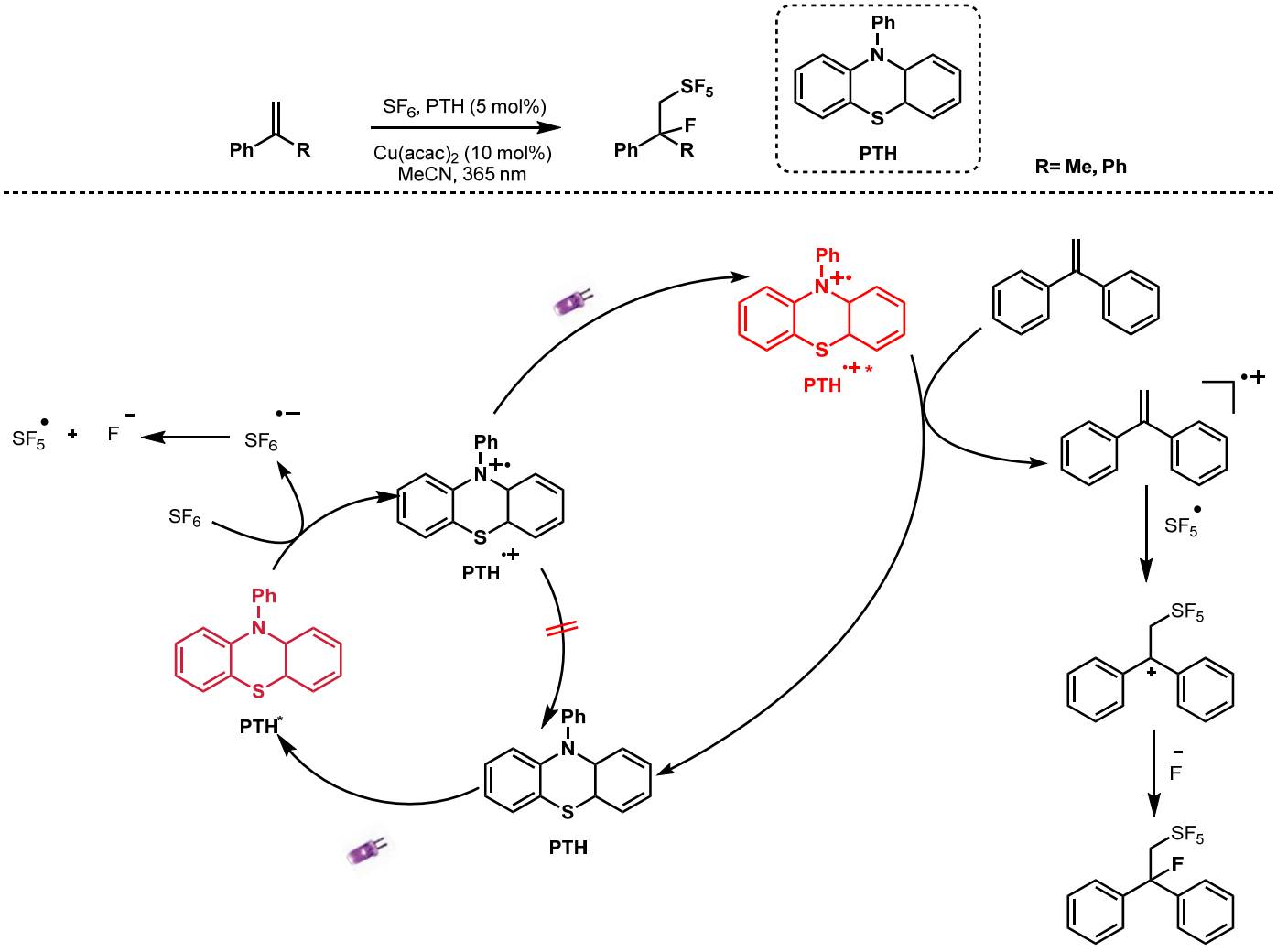

Rombach, D.; Wagenknecht, H.-A. *ChemCatChem* **2018**, *10*, 2955

Oxidations driven by ConPET processes

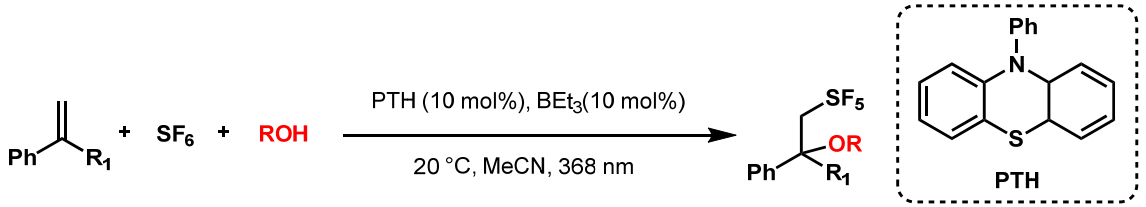

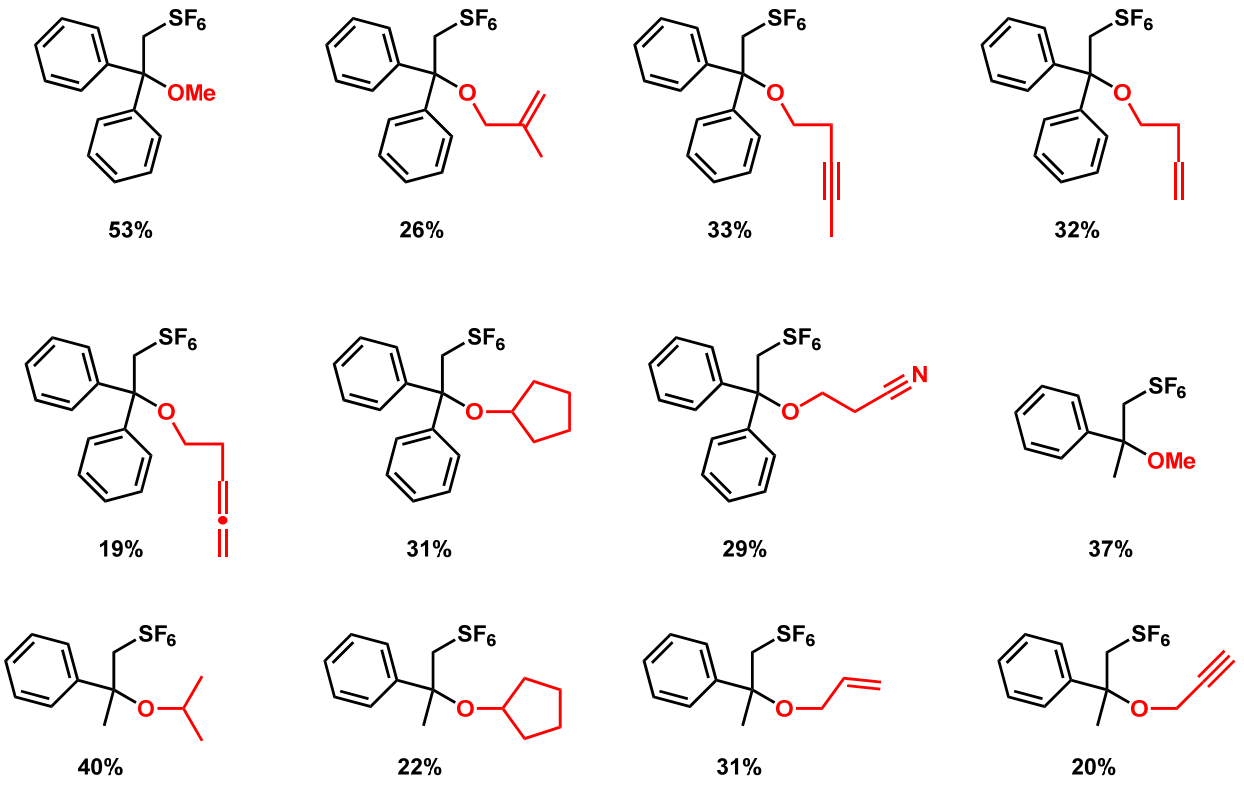

Rombach. D.; Wagenknecht, H.-A. *Angew. Chem. Int. Ed.* **2020**, *59*, 300

Oxidations driven by ConPET processes

Proposed mechanism

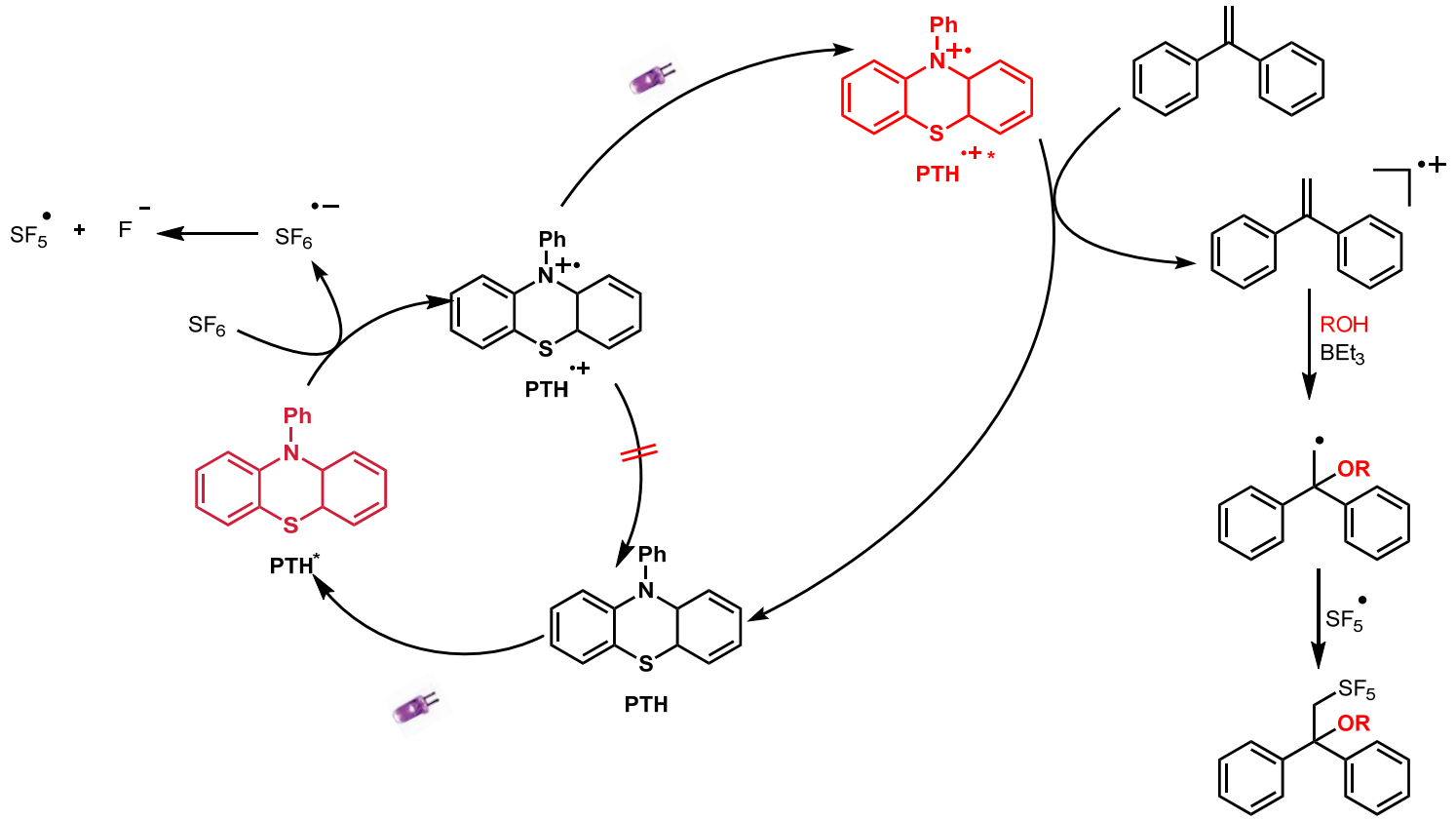

F^{-} can be captured by lewis acid, so the benzylic position can only be attacked by alcohols.

Rombach, D.; Wagenknecht, H.-A. *Angew. Chem. Int. Ed.* **2020**, *59*, 300

Oxidations driven by ConPET processes

Optimization of C–H amination

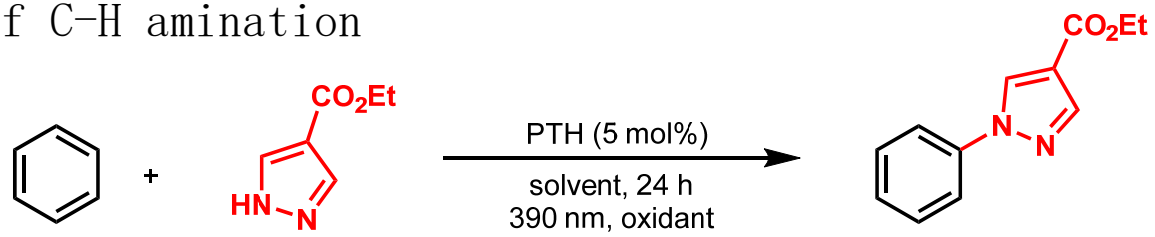

entry	oxidant	solvent	additive	yield (%)
1	none	MeCN	none	n.d.
2	PhI (2 equiv)	MeCN	none	n.d.
3	PhBr (2 equiv)	MeCN	none	2
4	CH_2Br_2 (2 equiv)	MeCN	none	5
5	$NOPF_6$ (2 equiv)	MeCN	none	12
6	$Cu(TFA)_2$ (2 equiv)	MeCN	none	n.d.
7	O_2 (1 atm)	MeCN	none	14
8	O_2 (1 atm)	TFE	none	31
9	O_2 (1 atm)	TFE : HFPI 9:1	$LiClO_4$ (20 mol%)	89

Targos, K.; Williams, O. P.; Wickens, Z. K. *J. Am. Chem. Soc.* **2021**, *143*, 4125

Oxidations driven by ConPET processes

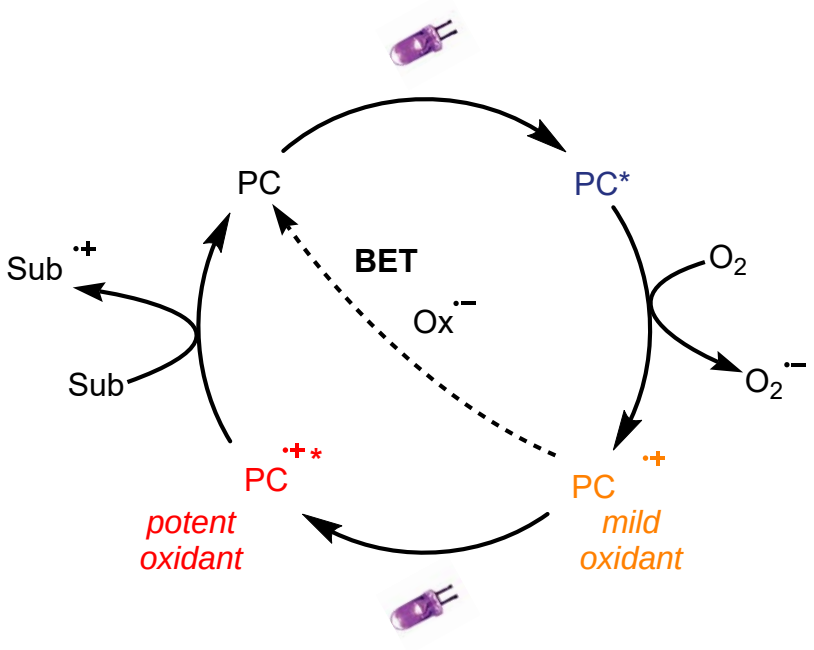

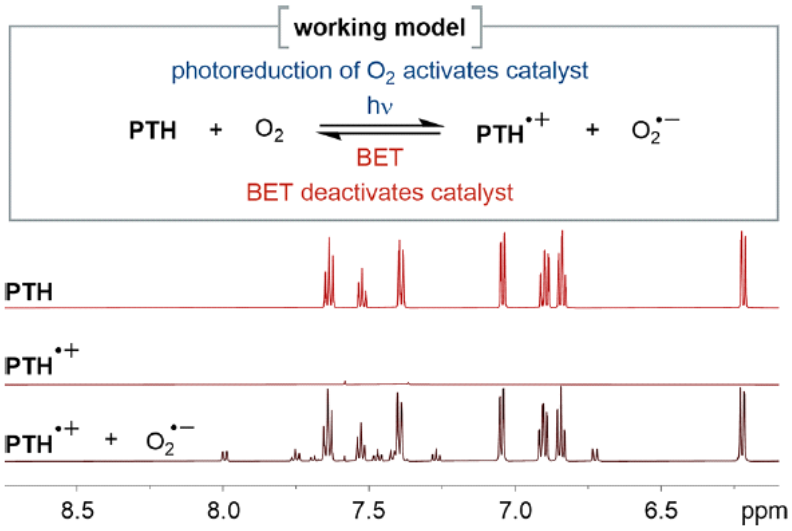

^{1}H NMR spectroscopic

The role of lithium perchlorate is to quench the superoxide.

BET: back electron transfer.

Targos, K.; Williams, O. P.; Wickens, Z. K. *J. Am. Chem. Soc*. **2021**, *143*, 4125

Oxidations driven by ConPET processes

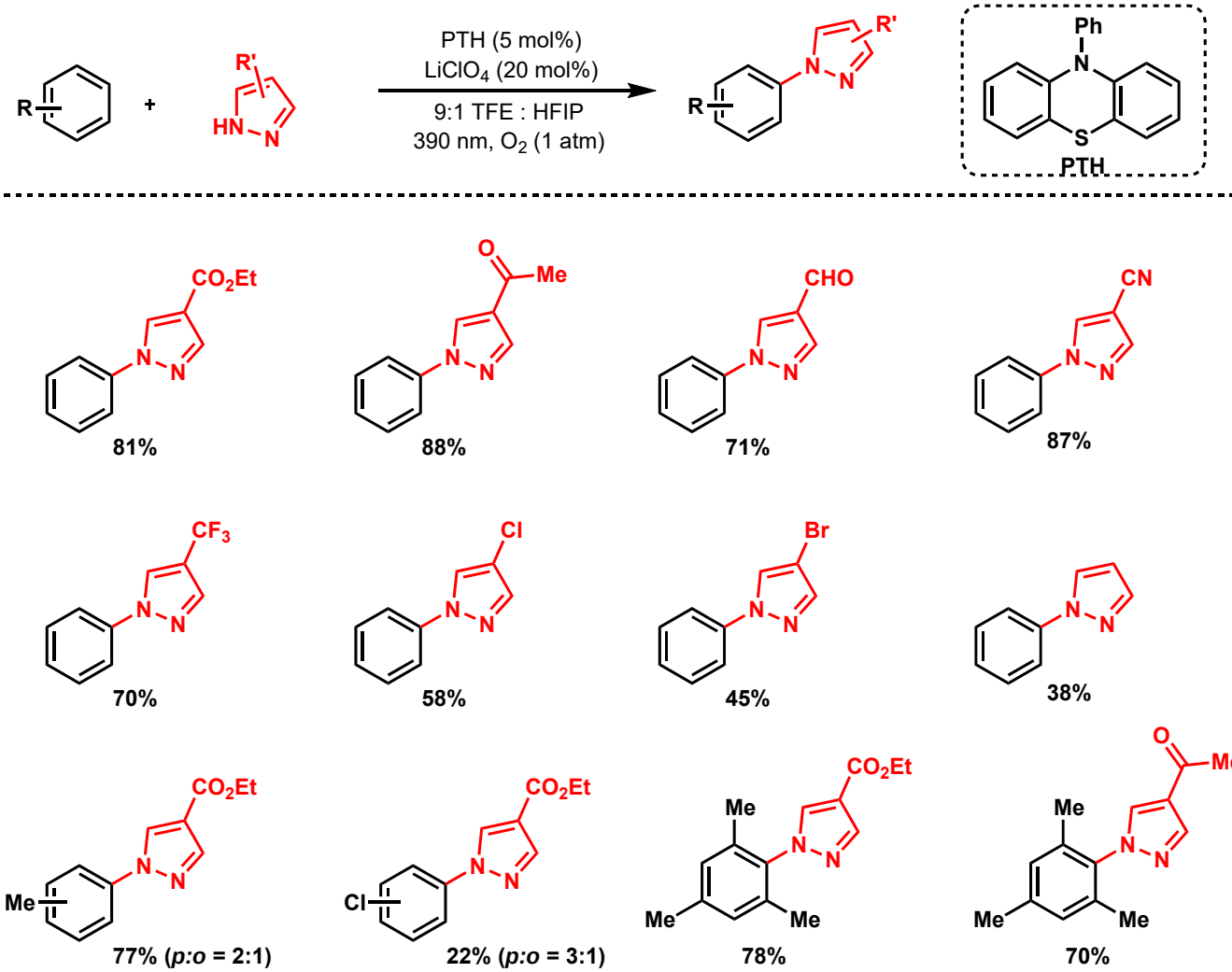

Targos, K.; Williams, O. P.; Wickens, Z. K. *J. Am. Chem. Soc.* **2021**, *143*, 4125

Content

Conclusion

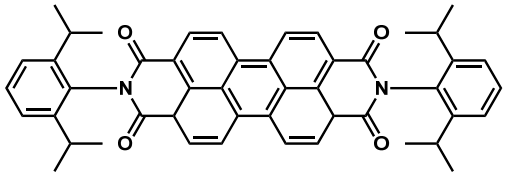

perylene diimide (**PDI**)

König Burkhard
Science **2014**, 725

dehalogenation
C-C bond-forming arylation

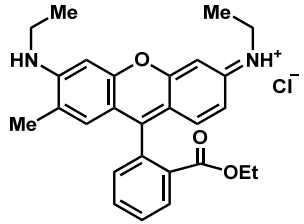

Rh-6G

König Burkhard
ACIE, **2016**, *55*, 7676

bond activation through light-color regulation

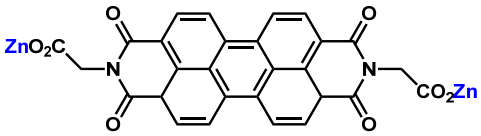

ZnPDI

Duan Chunying
JACS, **2016**, *138*, 3958

Heterogeneous catalysis

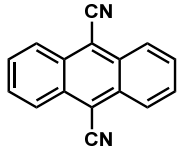

dicyanoanthracene (**DCA**)

Pérez-Ruiz Raul
Chem. Eur. J. **2018**, *24*, 105

C-C bond-forming arylation

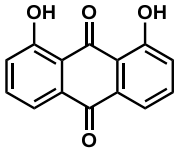

dihydroxyanthraquinone (**Aq-OH**)

König Burkhard
Eur. J. Org. Chem. **2018**, 34

dehalogenation

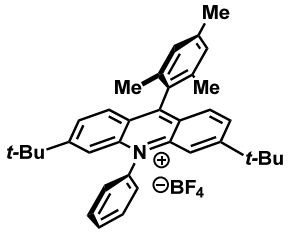

Mes-Acr-BF_4

Nicewicz David A.
Nature **2020**, 76

dehalogenation
detosylation

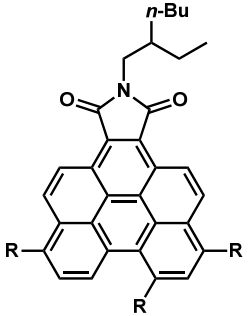

Benzo[ghi]perylene (**BPI**)

Miyake Garret M.
JACS, **2020**, *142*, 13573

birch reduction

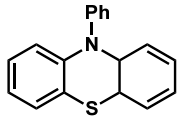

N-phenylphenothiazine (**PTH**)

ChemCatChem ***2018***, *10*, 2955;
ACIE, **2020**, *59*, 300;
JACS, **2021**, *143*, 4125

pentafluorosulfanylation
C-H amination

Thanks for your attention